

## **Two New Cryptic Endemic Toads of Bufo Discovered in Central Nevada, Western United States (Amphibia: Bufonidae: Bufo [Anaxyrus])**

Authors: Gordon, Michelle R., Simandle, Eric T., Sandmeier, Franziska C., and Tracy, C. Richard

Source: Copeia, 108(1) : 166-183

Published By: The American Society of Ichthyologists and Herpetologists

URL: <https://doi.org/10.1643/CH-18-086>

---

The BioOne Digital Library (<https://bioone.org/>) provides worldwide distribution for more than 580 journals and eBooks from BioOne's community of over 150 nonprofit societies, research institutions, and university presses in the biological, ecological, and environmental sciences. The BioOne Digital Library encompasses the flagship aggregation BioOne Complete (<https://bioone.org/subscribe>), the BioOne Complete Archive (<https://bioone.org/archive>), and the BioOne eBooks program offerings ESA eBook Collection (<https://bioone.org/esa-ebooks>) and CSIRO Publishing BioSelect Collection (<https://bioone.org/csiro-ebooks>).

Your use of this PDF, the BioOne Digital Library, and all posted and associated content indicates your acceptance of BioOne's Terms of Use, available at [www.bioone.org/terms-of-use](http://www.bioone.org/terms-of-use).

Usage of BioOne Digital Library content is strictly limited to personal, educational, and non-commercial use. Commercial inquiries or rights and permissions requests should be directed to the individual publisher as copyright holder.

---

BioOne is an innovative nonprofit that sees sustainable scholarly publishing as an inherently collaborative enterprise connecting authors, nonprofit publishers, academic institutions, research libraries, and research funders in the common goal of maximizing access to critical research.

## Two New Cryptic Endemic Toads of *Bufo* Discovered in Central Nevada, Western United States (Amphibia: Bufonidae: *Bufo* [*Anaxyrus*])

Michelle R. Gordon<sup>1</sup>, Eric T. Simandle<sup>2</sup>, Franziska C. Sandmeier<sup>3</sup>, and C. Richard Tracy<sup>1</sup>

**We describe two new cryptic species of *Bufo* within the subgenus *Anaxyrus* discovered in Central Nevada of the western United States. Our analyses revealed that these two localized endemic toads are genetically divergent and morphologically distinct, yet were concealed under the range of the broadly distributed western toad (*Bufo boreas*), which occurs throughout Nevada. The newly discovered species are close in geographic proximity to each other (albeit, in different hydrological basins) but have evolved unique morphological characters that are distinct from each other and distinctive from all allied taxa within the *B. boreas* species complex. The delimiting of these two rare toads emphasizes the link between taxonomic cryptic and inadequate conservation as these newly described species are vulnerable to extinction due to severely restricted geographic ranges, unknown population sizes, and dependency on rare, fragile wetland habitat, which is a limited resource within Nevada, the primary state that makes up the arid Great Basin. These two endemics join the Great Basin *B. boreas* species complex as imperiled new members, and our study demonstrates that our knowledge of anuran diversity is incomplete and that new discoveries can still be made, even in unlikely settings.**

AMPHIBIANS are among the rarest vertebrates in the Great Basin Desert, yet the western toad (*Bufo* [*Anaxyrus*] *boreas*) can be found throughout much of the region with a range that extends across the western United States. The *B. boreas* species complex, which includes the cosmopolitan *B. boreas*, plus four narrowly distributed endemics confined to the hydrologic Great Basin: *B. canorus*, *B. exsul*, *B. nelsoni*, and the newly described *B. williamsi* (Gordon et al., 2017) are examples of the unique aquatic-dependent taxa within this arid ecoregion. Previous analyses examining the genetic diversity and endemism within the *B. boreas* species complex have suggested that cryptic lineages are likely present within the western toad's broad geographic range, and that the current taxonomy does not accurately reflect the diversity of *B. boreas* (Stephens, 2001), particularly around the Great Basin (Goebel, 2005; Goebel et al., 2009; Switzer et al., 2009). In our recent molecular examination of Great Basin diversity of *B. boreas*, we confirmed the presence of cryptic species, such as *B. williamsi* and two other lineages described here, which were all concealed under the broad range of the western toad. Our extensive collection of morphological measurements of live toads allowed us to quantify significant features that further distinguish these new species from *B. boreas* and allied taxa within the regional *B. boreas* species complex. Here, we describe two new species and highlight the consequence of taxonomic cryptic of undescribed species, which are constrained to extremely limited ranges, as these newest novel discoveries have the smallest known geographic distributions within the *B. boreas* species complex. Like both *B. williamsi* and *B. exsul*, these new species are restricted to rare spring-fed wetlands, a habitat within the Great Basin that is vulnerable to habitat loss and exploitation, warranting urgent conservation initiatives to protect and preserve these rare bufonids.

### MATERIALS AND METHODS

**Data collection and morphological analyses.**—We recorded morphological measurements from live adult toads from 19 populations within the hydrological Great Basin (Fig. 1A) including *B. boreas* ( $n = 289$ ), *B. exsul* ( $n = 30$ ), *B. nelsoni* ( $n = 31$ ), *B. williamsi* ( $n = 76$ ), plus individuals from both Hot Creek ( $n = 42$ ) and Railroad Valley ( $n = 50$ ) to comprise a large data set ( $n = 518$ ). Fourteen morphological features were recorded and are as follows: snout–vent length (SVL; tip of snout to posterior end of urostyle), head length (HL; tip of snout to occiput), head width (HW; at widest part of the head), snout length (SL; tip of snout to anterior corner of eye), internarial distance (IND; distance between nares), eye diameter (ED; at widest part of eye), interorbital space (IOD; shortest distance between medial margin of upper eyelids), tympanum diameter (TYM; at maximum width of tympanum), paratoid length (PL; horizontal length of paratoid gland) and width (PW; maximum width of paratoid), interparatoid distance (IPD; shortest distance between medial margin of paratoid glands), femur length (FL; distance between vent and knee), tibial length (TL; distance between knee and heel), and hind foot length (FTL; distance from anterior margin of heel to distal end of the third toe). All morphological characteristics were measured using Mitutoyo digital calipers to a precision of 0.1 mm. All individuals were measured by ETS with the exception of 13 individuals collected from Hot Creek and 19 individuals collected from Railroad Valley, which were measured by MRG, including the holotypes and paratypic series from each site. Digit length from hands and forelimbs were recorded by MRG. Sex was determined in the field, noting body size, behavior, and secondary sex characteristics, such as the utilization of a release call and presence of nuptial pads on males as identifiers.

<sup>1</sup> Department of Biology, University of Nevada, Reno, Reno, Nevada 89557; Email: (CRT) dtracy@unr.edu. Send reprint requests to CRT.

<sup>2</sup> Department of Geography, University of Nevada, Reno, Reno, Nevada 89557.

<sup>3</sup> Department of Biology, Colorado State University–Pueblo, Pueblo, Colorado 81001-4901.

Submitted: 4 July 2018. Accepted: 19 November 2019. Associate Editor: B. Stuart.

© 2020 by the American Society of Ichthyologists and Herpetologists DOI: 10.1643/CH-18-086 Published online: 27 March 2020

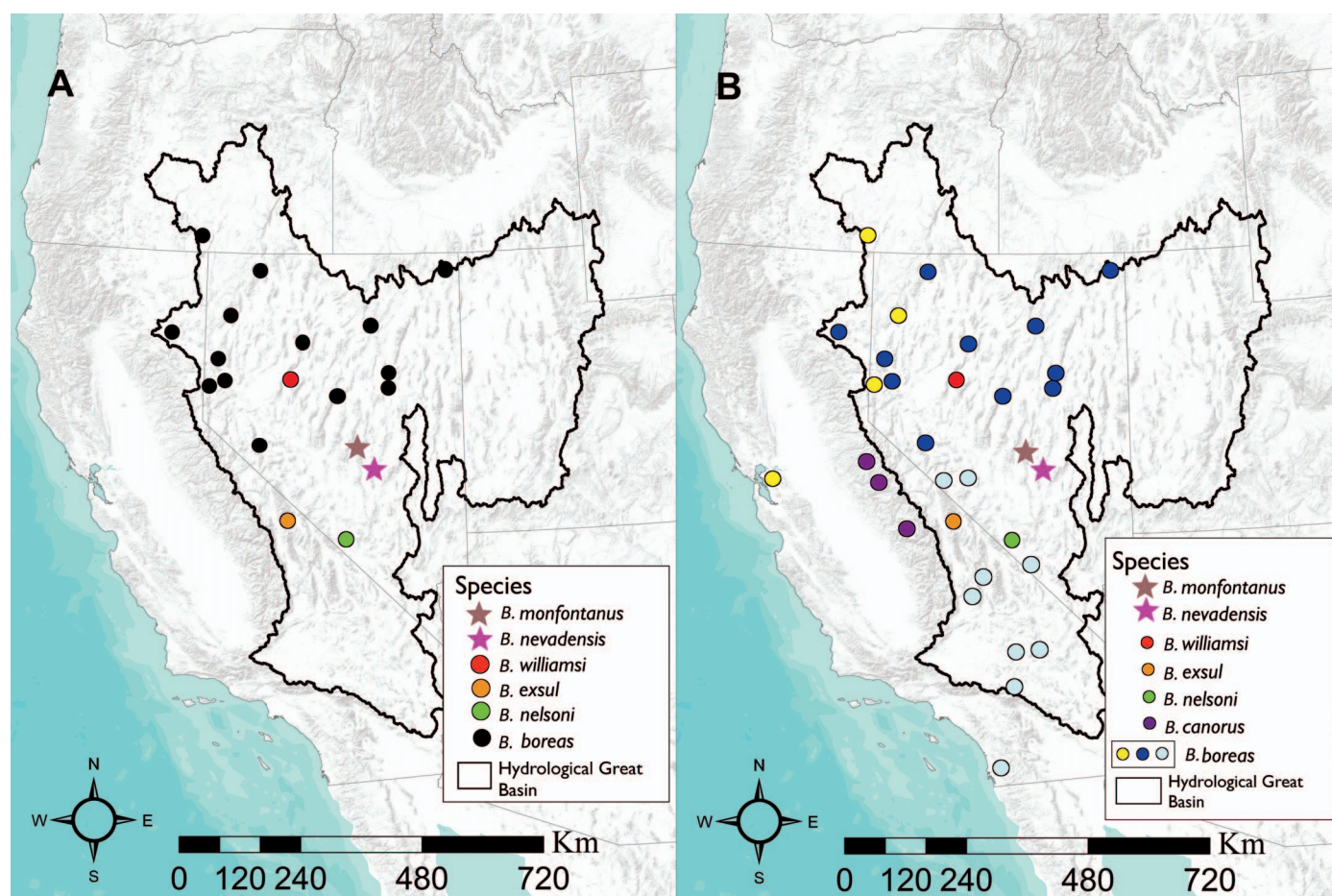


**Fig. 1.** Sampling localities of congeneric taxa within the *B. boreas* species complex included for morphological (A) and DNA (B) collections within the hydrological Great Basin and surrounding states (Gordon et al., 2017). (A) Colors indicate species-specific populations measured for morphological analysis, with stars denoting new species. (B) Colors correspond with localized species and colors of *B. boreas* correspond with major mtDNA haplotype clades: W—Oregon and Western Great Basin (yellow), HL—Humboldt-Lahontan (blue), S—Mojave (aqua), and stars denote new species, which comprise the Eastern Great Basin clade (E). Maps created using ArcGIS software by ESRI (Environmental Systems Research Institute, 2011, ArcGIS Desktop: Release 10. Redlands, CA).

Individuals collected in May of 2015 from populations in Hot Creek Canyon and the eastern neighboring basin, Railroad Valley, were selected to represent the holotypes and paratype series for both species and were euthanized and preserved following the guidelines under the Institutional Animal Care and Use Committee (IACUC) from University of Nevada (IACUC #00068). The extracted tissue samples were preserved and deposited at the University of Nevada, Reno (UNR). Specimens were fixed in 10% buffered formalin and transferred to 70% ethanol and deposited as vouchers in the California Academy of Science (CAS) and University of Nevada, Reno.

To characterize morphological differences among species, we used multivariate analysis of covariance (MANCOVA) and used SVL as the covariate in these analyses to account for body-size variability among species (Dahl and Peckarsky, 2002; McCoy et al., 2006). This analysis results in least squares means generated from regressions for each size corrected variable against SVL, which can identify subtle, but statistically significant differences in fine features examined in these toads. We also log transformed the raw dataset as an additional way to account for differences in allometry of measured toads and analyzed the scaled data set using MANCOVA to quantify morphological differences

among the species (Lleonart et al., 2000). We used Tukey HSD *post hoc* pairwise comparisons to identify significant character state differences among the species examined (Feinberg et al., 2014). A cross-validated discriminant function analysis (DFA) was used to evaluate the variation in multivariate space to identify variables that best discriminated among the species (Feinberg et al., 2014). Data collected from multiple measurers can result in inter-observer error due to variations in character assessment, particularly on the fine features of amphibian anatomy (Hayek et al., 2001). These errors can produce results that may bias biological interpretations from morphological analyses (Hayek et al., 2001). To avoid inter-observer biases, only measurements collected by ETS were used in the morphological analyses with the exception of the means table (Table 1), which includes combined raw, unadjusted measurements from ETS and MRG. All statistics were conducted using JMP Pro v. 10 (SAS, Cary, NC).

**Genetics.**—Following the methods described in Gordon et al. (2017), tissue samples were collected from individuals identified as *B. boreas* (Fig. 1B;  $n = 308$ ), *B. canorus* ( $n = 32$ ), *B. exsul* ( $n = 30$ ), *B. nelsoni* ( $n = 32$ ), and *B. williamsi* ( $n = 7$ ). The control region (CR) of the mitochondrial genome was



**Table 1.** Morphological variation of six species that comprise the *B. boreas* species complex of the Great Basin. Fourteen morphological measurements (in mm) are as follows: snout–vent length (SVL), head length (HL), head width (HW), snout length (SL), internarial distance (IND), eye diameter (ED), interorbital distance (IOD), tympanum diameter (TYM), parotoid width (PW), parotoid length (PL), interparotoid distance (IPD), femur length (FL), tibial length (TL), and foot length (FTL). Data include sample size (*n*), character mean  $\pm$  standard deviation, and range. All measurements reflect raw, unadjusted values.

	Holotype <i>B. nevadensis</i>	Holotype <i>B. monfontanus</i>	<i>B. nevadensis</i> ( <i>n</i> = 50)	<i>B. monfontanus</i> ( <i>n</i> = 42)	<i>B. boreas</i> ( <i>n</i> = 289)	<i>B. nelsoni</i> ( <i>n</i> = 31)	<i>B. exsul</i> ( <i>n</i> = 30)	<i>B. williamsi</i> ( <i>n</i> = 76)
SVL	62.5	59.6	63.7 $\pm$ 6.1	60.2 $\pm$ 4.2	82.3 $\pm$ 12.2	80.8 $\pm$ 13.0	64.0 $\pm$ 8.4	54.6 $\pm$ 4.7
range			47.3–75.0	50.0–69.0	53.0–113.0	57.0–122.0	53.0–79.0	44.0–70.0
HL	17.2	16.2	18.6 $\pm$ 2.6	17.2 $\pm$ 1.7	24.0 $\pm$ 3.0	24.0 $\pm$ 3.3	18.6 $\pm$ 2.4	16.0 $\pm$ 1.6
range			13.5–22.3	13.0–19.8	16.9–30.9	17.2–31.8	15.0–22.9	11.6–20.0
HW	20.1	19.3	21.3 $\pm$ 2.1	20.4 $\pm$ 1.5	27.6 $\pm$ 3.9	28.1 $\pm$ 4.4	20.6 $\pm$ 3.0	18.2 $\pm$ 1.5
range			15.7–24.2	17.1–23.4	18.5–36.21	19.0–37.7	16.6–25.0	14.8–24.3
SL	7.5	6.4	5.2 $\pm$ 1.5	5.2 $\pm$ 1.0	5.6 $\pm$ 0.8	5.4 $\pm$ 0.8	4.4 $\pm$ 0.7	5.4 $\pm$ 0.9
range			3.2–8.6	3.7–7.6	3.7–8.4	4.5–7.6	3.3–6.2	3.9–7.4
IND	3.8	2.3	4.0 $\pm$ 1.0	3.9 $\pm$ 0.8	5.0 $\pm$ 0.6	5.2 $\pm$ 0.7	4.3 $\pm$ 0.5	3.2 $\pm$ 0.9
range			1.6–5.2	2.2–5.7	3.1–6.7	4.0–7.2	3.1–5.6	1.5–4.6
ED	4.8	4.4	5.9 $\pm$ 1.1	5.5 $\pm$ 0.8	7.5 $\pm$ 1.0	7.6 $\pm$ 1.1	6.0 $\pm$ 0.7	5.8 $\pm$ 0.9
range			3.4–7.7	3.5–6.5	4.7–10.3	5.4–10.9	4.7–7.1	3.2–7.7
IOD	4.8	3.8	3.2 $\pm$ 0.8	3.5 $\pm$ 0.6	12.9 $\pm$ 1.7	12.2 $\pm$ 2.0	9.7 $\pm$ 1.0	5.4 $\pm$ 3.2
range			1.9–5.0	2.6–4.6	9.1–17.8	9.3–18.7	7.8–11.9	1.7–10.6
TYM	3.0	2.5	2.7 $\pm$ 0.6	2.7 $\pm$ 0.4	4.9 $\pm$ 0.8	4.2 $\pm$ 0.7	3.2 $\pm$ 0.3	2.8 $\pm$ 0.5
range			1.5–3.8	1.5–3.6	2.4–6.6	3.2–5.6	2.7–4.2	1.8–3.9
PW	3.7	5.3	4.8 $\pm$ 0.7	5.7 $\pm$ 0.5	7.1 $\pm$ 1.1	6.9 $\pm$ 1.0	5.4 $\pm$ 0.8	5.2 $\pm$ 0.8
range			3.4–6.1	4.5–6.5	4.5–10.6	5.1–9.5	3.8–6.5	3.4–7.4
PL	7.5	8.8	6.8 $\pm$ 0.91	8.7 $\pm$ 0.9	10.0 $\pm$ 1.6	8.8 $\pm$ 1.3	6.8 $\pm$ 0.9	6.5 $\pm$ 1.0
range			4.6–8.9	6.7–10.6	6.6–14.6	5.7–11.5	5.5–8.8	4.2–9.5
IPD	12.3	9.4	12.1 $\pm$ 1.7	10.9 $\pm$ 1.3	15.8 $\pm$ 2.4	15.6 $\pm$ 2.7	11.9 $\pm$ 1.5	10.4 $\pm$ 1.1
range			8.9–15.0	8.7–16.0	11.0–23.0	11.5–23.0	10.0–15.0	8.2–14.0
FL	21.2	23.1	24.9 $\pm$ 3.4	20.8 $\pm$ 1.8	32.8 $\pm$ 4.4	31.1 $\pm$ 4.6	24.5 $\pm$ 3.3	19.6 $\pm$ 2.7
range			16.5–29.0	15.0–23.1	22.0–44.0	20.0–41.0	19.0–30.0	14.2–27.0
TL	18.7	19.7	23.6 $\pm$ 4.2	20.9 $\pm$ 2.9	32.2 $\pm$ 4.4	30.3 $\pm$ 4.6	24.2 $\pm$ 3.4	18.2 $\pm$ 2.7
range			14.1–28.0	14.3–25.0	22.0–43.0	19.0–38.0	18.0–29.0	13.2–24.0
FTL	37.0	35.0	30.5 $\pm$ 4.0	27.7 $\pm$ 4.7	33.8 $\pm$ 4.4	32.6 $\pm$ 5.0	26.2 $\pm$ 3.8	26.5 $\pm$ 4.2
range			24.5–39.4	19.0–37.7	21.0–44.0	23.0–45.0	19.0–31.0	19.0–38.7

selected due to the region's high rate of evolution ideal for intraspecific analyses (Avise et al., 1987) and because it has been used in previous phylogenetic studies evaluating the diversity in *B. boreas* (Stephens, 2001; Goebel et al., 2009). Primers were modified using previously published sequences (Goebel et al., 1999; Stephens, 2001) to amplify approximately 1,622 bp area of the CR (Table 2). PCR products were sequenced using ABI 3730 sequencer, and data were analyzed with Sequencher software (Gene Codes, Ann Arbor, MI). The final alignment of the *B. boreas* species complex (CR 1,622 bp) was completed using ClustalW (Larkin et al., 2007) within Mega 7.0 (Kumar et al., 2016), resulting in 62 unique haplotypes included in further analyses. Haplotype, locality, species, and GenBank accession numbers are in Table 3. To examine pairwise genetic distances among sequences relative to haplotypes identified, a Jukes-Cantor model (Jukes and Cantor, 1969) was applied in Mega 7.0 (Kumar et al., 2016).

**Genetic analyses.**—Previous molecular studies support evidence of recent divergence of allied taxa within the *B. boreas* species complex (Feder, 1973; Graybeal, 1993; Shaffer et al., 2000; Stephens, 2001; Pauly et al., 2004; Goebel et al., 2009; Switzer et al., 2009). Due to the close ancestry of this species group, we constructed a TCS haplotype network in PopART to examine population level genealogy (Clement et al., 2002; Leigh and Bryant, 2015). Phylogenetic hypotheses were

tested using Bayesian inference (BI) in MrBayes v3.1.2 (Ronquist and Huelsenbeck, 2003) using parameters described in Gordon et al. (2017). The program Tracer v1.6 (Rambaut et al., 2014) confirmed that analyses reached stationarity and trees were constructed using FigTree v1.4.2 (Rambaut, 2014). Maximum likelihood (ML) phylogenies were constructed in Mega 7.0 (Kumar et al., 2016) to examine evolutionary relationships and comparative tree topologies among taxa of the *B. boreas* species complex. The evolutionary history was inferred based on the Hasegawa-Kishino-Yano model (Hasegawa et al., 1985) suggested by Akaike Information Criterion (AIC; Burnham and Anderson, 2002), and support was evaluated using 500 bootstrap replications (Pattengale et al., 2010). A discrete gamma distribution was used to model evolutionary rate differences among sites (5 categories [+G, parameter = 0.6336]). *Bufo punctatus* was selected as the outgroup since this taxon was included in previous studies that examined the same molecular marker investigating the fine-scale relationship of toads within the *B. boreas* species complex (Stephens, 2001; Goebel et al., 2009). All positions containing gaps and missing data were eliminated. There were a total of 1,401 positions in the final dataset.

To examine the relationships of populations of *B. boreas* outside the Great Basin to the variant haplotypes for a broader geographic and historical context, sequences for the

**Table 2.** Primers used to amplify the mitochondrial control region (CR) in *B. boreas* and *B. punctatus*.

Primer name	Species	PCR or Seq primer	Sequence 5' to 3'
Bmt14844F	<i>Bufo boreas</i>	PCR/Seq	ACG CCA TCC TTC GAT CTA TTC
Bmt14999R	<i>Bufo boreas/B. punctatus</i>	Seq	AGT GAG GAT GAG TGT GTT AGC
Bmt14223F	<i>Bufo boreas/B. punctatus</i>	PCR/Seq	TGT TAT GAT TGG TCA ATT AGC
Bmt15400R	<i>Bufo boreas</i>	Seq	GCG ATG ACA GAG GGT TTA GTG
Bmt15273F	<i>Bufo boreas</i>	Seq	ATT CAC CTT ACT TCC CCA TGC
Bmt15612R	<i>Bufo boreas/B. punctatus</i>	PCR/Seq	ATT AAG ATC ATT CCA TCT TCG
Bmt15777F	<i>Bufo boreas/B. punctatus</i>	PCR/Seq	TAT TAT TGA ACA ATC TCA GCC
Bmt15930R	<i>Bufo boreas/B. punctatus</i>	PCR/Seq	ATA AGT ATT ATT CGT ATT GAC
Bmt16207F	<i>Bufo boreas/B. punctatus</i>	PCR/Seq	TAC TTA GAA ATT CTC TAC ACC
Bmt16237R	<i>Bufo boreas/B. punctatus</i>	PCR/Seq	GAG GGA GGC TCT TTA GAT TTC
Bmt14200R	<i>Bufo boreas/B. punctatus</i>	PCR/Seq	AAG AAG AGG CTC TTT GAC GGG
Bmt15421F	<i>Bufo punctatus</i>	PCR/Seq	CAT GCA TAT CAT CAC CAA TGC
Bmt14835F	<i>Bufo punctatus</i>	Seq	ATA CTT TCT ATT TGC CTA CGC
Bmt14743F	<i>Bufo punctatus</i>	PCR/Seq	TTA TCC ACC TTC GCC CC
Bmt15854R	<i>Bufo punctatus</i>	Seq	TAT TAG ATT GAC CAT GGA TGG
Bmt15000F	<i>Bufo punctatus</i>	Seq	CAC AGA GAA CAA GCT AGC TCG
Bmt15795F	<i>Bufo punctatus</i>	Seq	AAC TGG ACC TGA AAG TCC TAG
Bmt16155R	<i>Bufo punctatus</i>	Seq	AGT TAA GGT CTT TAA GGT ACC
Bmt14877F	<i>Bufo punctatus</i>	PCR/Seq	CAA ACT GGG AGG AGT CCT AGC
Bmt15100R	<i>Bufo punctatus</i>	PCR/Seq	TAA GAT TAC TCT GTA GAG TCG
Bmt15050F	<i>Bufo punctatus</i>	PCR/Seq	TAC ATC CCT ACA TCA TAA TCG
Bmt15500R	<i>Bufo punctatus</i>	PCR/Seq	ATG TGG AAG GTA TTC ATA AGC
Bmt15335F	<i>Bufo punctatus</i>	PCR/Seq	TAG GGG ACA TAT TAT TAA TGC
Bmt15863R	<i>Bufo punctatus</i>	PCR/Seq	GTT TGT GTT TAT TAG ATT GGC

control region from Goebel et al. (2009) were downloaded from GenBank and added to the dataset (Table 3) in Mega 7.0 (Kumar et al., 2016). To reconstruct the evolutionary history, 87 unique haplotypes were used in ML based on the Hasegawa-Kishino-Yano model (Hasegawa et al., 1985). All positions containing gaps and missing data were eliminated. There were a total of 628 positions in the final dataset using ML in Mega 7.0 (Kumar et al., 2016).

## RESULTS

**Morphological evidence.**—There were significant differences for all 14 size-corrected morphological characters among *B. boreas*, *B. exsul*, *B. nelsoni*, *B. williamsi*, and populations of Hot Creek (*Bufo monfontanus*, new species) and Railroad Valley (*Bufo nevadensis*, new species). *Bufo nevadensis*, new species, is significantly smaller overall than larger bufonids *B. boreas* and *B. nelsoni* ( $F_{5,439} = 62.4$ ,  $P < 0.0001$ ), yet it has a significant, but modestly larger head ( $F_{6,439} = 704.0$ ,  $P < 0.0001$ ;  $F_{6,439} = 899.6$ ,  $P < 0.0001$ ; Table 4), which is longer than similar body-sized congeners, *B. exsul*, *B. monfontanus*, new species, and *B. williamsi*, with moderate, well-separated eyes ( $F_{6,439} = 290.1$ ,  $P < 0.0001$ ). Significant differences were detected among species for snout length ( $F_{6,439} = 145.8$ ,  $P < 0.0001$ ), and in pairwise comparisons recovered from Tukey HSD *post hoc* tests (Table 4), *B. nevadensis*, new species, has a short snout, which, while perceptibly subtle, differs significantly from all other congeners examined in this study except *B. exsul*. The parotoid glands of *B. nevadensis*, new species, are significantly reduced; parotoid width is narrower than all congeners examined ( $F_{6,439} = 145.1$ ,  $P < 0.0001$ ) and shorter in length than *B. boreas* and *B. monfontanus*, new species ( $F_{6,439} = 156.6$ ,  $P < 0.0001$ ; Table 4). Additionally, the small-sized *B. nevadensis*, new species, has relatively long legs; the femur is comparatively longer than all other congeners

with the exception of the larger toads *B. boreas* and *B. nelsoni* ( $F_{6,439} = 741.2$ ,  $P < 0.0001$ ; Table 4), and tibial and foot length are longer than the similar-sized toads *B. williamsi* and *B. monfontanus*, new species ( $F_{6,439} = 770.8$ ,  $P < 0.0001$ ;  $F_{6,439} = 392.3$ ,  $P < 0.0001$ ; Table 4).

*Bufo monfontanus*, new species, has a significantly smaller body size than the larger sized toads, *B. boreas* and *B. nelsoni* ( $F_{5,439} = 62.4$ ,  $P < 0.0001$ ; Table 4), and outsizes only *B. williamsi* (Tables 1, 4). This small toad has a wide head similar to *B. boreas* and *B. nevadensis*, new species, but it has the shortest relative head length of all species within the complex ( $F_{6,439} = 899.6$ ,  $P < 0.0001$ ; Table 4), with moderate, well-separated eyes ( $F_{6,439} = 290.1$ ,  $P < 0.0001$ ; Table 4). Significant differences in parotoid width were detected among the species complex ( $F_{6,439} = 145.1$ ,  $P < 0.0001$ ) and in pairwise comparisons in Tukey HSD *post hoc* tests, *B. monfontanus*, new species, exhibits the longest parotoid gland, which differs significantly, though the physical difference is modest, from all congeners of the complex except *B. boreas* ( $F_{6,439} = 156.6$ ,  $P < 0.0001$ ; Table 4). The large glands are comparatively closer together, which is significantly different from that presented in *B. boreas*, *B. nelsoni*, and *B. nevadensis*, new species ( $F_{6,439} = 380.2$ ,  $P < 0.0001$ ; Table 4). The leg features of *B. monfontanus*, new species, are reduced with significant differences detected; while perceptibly subtle, *B. monfontanus*, new species, has the shortest femur among all congeners of the complex ( $F_{6,439} = 741.2$ ,  $P < 0.0001$ ; Table 4), shorter tibia differing from lengths observed in *B. boreas*, *B. nelsoni*, and the small toad, *B. nevadensis*, new species ( $F_{6,439} = 770.8$ ,  $P < 0.0001$ ; Table 4), and a small foot length distinct from *B. boreas* and *B. nevadensis*, new species ( $F_{6,439} = 392.3$ ,  $P < 0.0001$ ; Table 4).

In multivariate morphospace using DFA, significant differences were detected among species ( $F_{70,323} = 3.40$ ,  $P <$

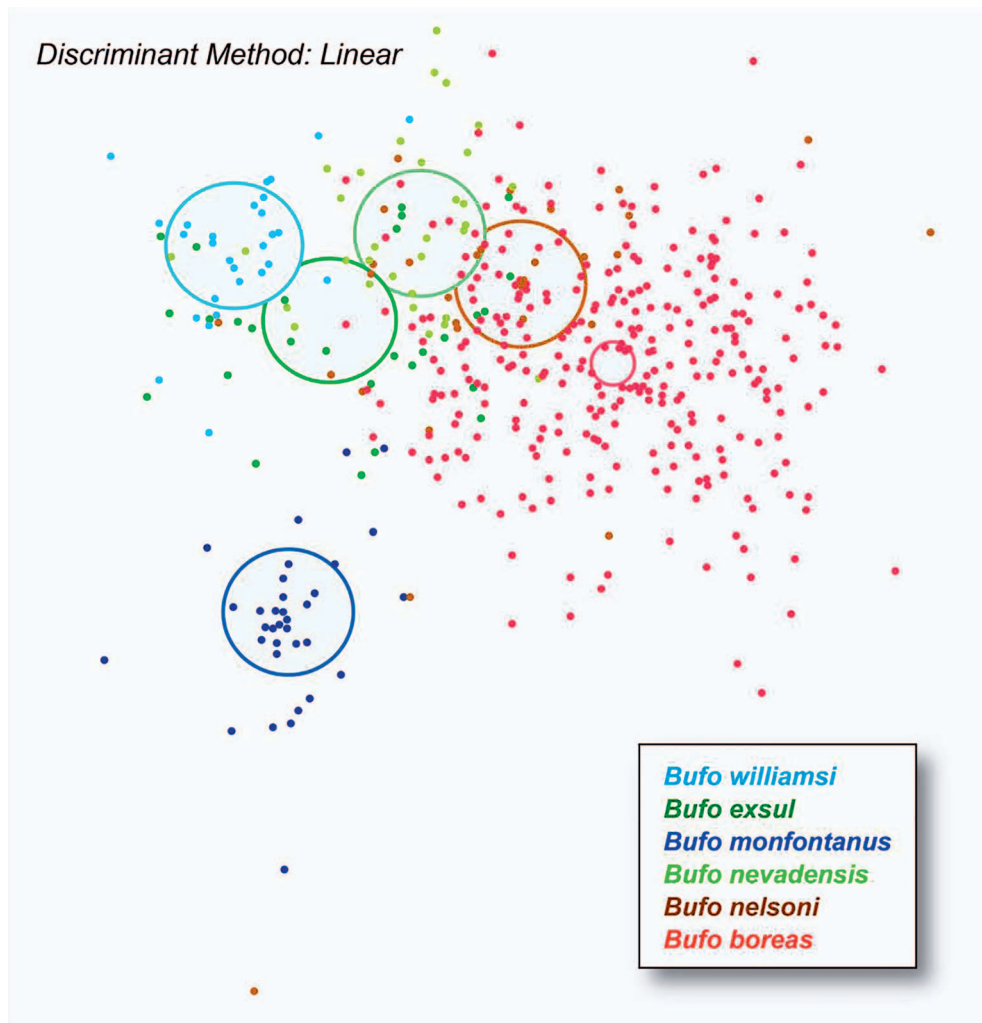


**Fig. 2.** Discriminant function analysis (DFA). Cross validated DFA using 14 size-corrected morphological characters measured from 518 live adult toads (Fig. 1A) examined within the hydrological Great Basin *B. boreas* species complex. Species identified as *B. boreas* (red), *B. nelsoni* (brown), *B. exsul* (dark green), *B. williamsi* (light blue), *B. nevadensis* (light green), and *B. monfontanus* (dark blue).

0.0001; Fig. 2). The DFA correctly classified 83.7% of predicted species with some morphological overlap detected among *B. boreas*, *B. exsul*, *B. nelsoni*, and *B. nevadensis*, new species. Little morphological overlap was detected with *B. monfontanus*, new species. Canonical 1 explained 61% of the variation with head width loading most heavily, while canonical 2 accounted for 17% of the variation with parotoid length loading more heavily than other characters (Fig. 2).

To assess sexual dimorphism in *B. monfontanus*, new species (females = 16, males = 13), and *B. nevadensis*, new species (females = 28, males = 3), intraspecific analyses showed significant differences in SVL detected only in *B. monfontanus*, new species ( $F_{1,28} = 5.4$ ,  $P < 0.03$ ), with females significantly larger than males ( $P < 0.05$ ). However, males of *B. monfontanus*, new species, have relatively longer legs than females ( $F_{2,28} = 12.7$ ,  $P < 0.0001$  for femur length;  $F_{2,28} = 24.1$ ,  $P < 0.0001$  for tibial length;  $F_{2,28} = 19.0$ ,  $P < 0.0001$  for foot length). While sexual dimorphism was not detected in SVL of *B. nevadensis*, new species ( $F_{1,30} = 1.2$ ,  $P = 0.28$ ), males did have relatively longer feet ( $F_{2,30} = 8.4$ ,  $P < 0.001$ ). The unadjusted data collected for the six species examined for all 14 characters are presented in Table 1.

**Genetic evidence and phylogenetic relationships.**—Similar to the findings presented by Gordon et al. (2017), the combined analyses for the control region of the mitochondrial genome

examined in the *B. boreas* species complex study supported the existence of divergent lineages of undefined toad populations within the Great Basin, warranting inspection of cryptic populations occurring in Central Nevada and described herein. The TCS haplotype network and phylogenetic reconstructions support four major clades that correspond roughly to geographical regions within the hydrological Great Basin and defined as Western Great Basin (W), Humboldt-Lahontan (HL), Mojave (S), and Eastern Great Basin (E; Figs. 1B, 3, 4, Supp. Figs. 1, 2; see Data Accessibility). The haplotype network highlights the divergent lineages of *B. monfontanus*, new species, and *B. nevadensis*, new species, from each other and to all *B. boreas* within the hydrological Great Basin (Fig. 3A) and illustrates the regional divide in diversity among populations of *B. boreas* and related taxa within the species complex (Figs. 1B, 3). All phylogenies resulted in minor topological differences, but all results supported the divergence of the eastern Great Basin, which includes the newly described species *B. monfontanus*, new species, and *B. nevadensis*, new species, forming terminal taxa, and which are distinct from all congeners of the *B. boreas* species complex (Figs. 3B, 4, Supp. Figs. 1, 2; see Data Accessibility). In all combined analyses, the Mojave clade represents the most species-rich region of the Great Basin, with *B. exsul* and *B. nelsoni* plus haplotypes of both *B. canorus* and *B. boreas*. *Bufo boreas* and *B. canorus*



**Table 3.** Mitochondrial control region sequence data for *B. boreas* species complex. Haplotype, locality, species, and GenBank accession number. Sequences from Colorado and Utah were downloaded from GenBank (Goebel et al., 2009) with specimen locality and corresponding accession number for *B. boreas* DNA data.

Haplotype code	Taxon	Locality	GenBank accession numbers for CR1600 ( <i>n</i> = 62)
H1_521M	<i>Bufo canorus</i>	Short Hair Meadow, CA	MK284933
H2_521M2	<i>Bufo canorus</i>	Short Hair Meadow, CA	MK284934
H3_AF50	<i>Bufo boreas</i>	Afton Canyon, CA	MK284935
H4_AT206	<i>Bufo nelsoni</i>	Beatty, NV	MK284936
H5_BC10	<i>Bufo boreas</i>	Bouquet Canyon, CA	MK284937
H6_BC11	<i>Bufo boreas</i>	Bouquet Canyon, CA	MK284938
H7_BC16	<i>Bufo boreas</i>	Bouquet Canyon, CA	MK284939
H8_BC3	<i>Bufo boreas</i>	Bouquet Canyon, CA	MK284940
H9_BC9	<i>Bufo boreas</i>	Bouquet Canyon, CA	MK284941
H10_BT100	<i>Bufo exsul</i>	Deep Springs Valley, CA	MK284942
H11_BT104	<i>Bufo exsul</i>	Deep Springs Valley, CA	MK284943
H12_BWA	<i>Bufo boreas</i>	Alameda County, CA	MK284944
H13_SL17	<i>Bufo boreas</i>	Swan Lake, NV	MK284945
H14_SL1	<i>Bufo boreas</i>	Swan Lake, NV	MK284946
H20_Canor3	<i>Bufo canorus</i>	South Fork Merced, CA	MK284947
H21_Canor4	<i>Bufo canorus</i>	Ershim Meadow, CA	MK284948
H22_CD1	<i>Bufo boreas</i>	Cold Creek Reservoir, NV	MK284949
H23_CL1	<i>Bufo boreas</i>	China Lake, CA	MK284950
H24_DF10	<i>Bufo boreas</i>	Darwin Falls, CA	MK284951
H25_DX2	<i>Bufo williamsi</i>	Dixie Valley, NV	MK284952
H26_EL1	<i>Bufo boreas</i>	Eagle Lake, CA	MK284953
H27_EL15	<i>Bufo boreas</i>	Eagle Lake, CA	MK284954
H28_EML02	<i>Bufo canorus</i>	Emmigrant Meadow, CA	MK284955
H29_EML03	<i>Bufo canorus</i>	Emmigrant Meadow, CA	MK284956
H30_EML05	<i>Bufo canorus</i>	Emmigrant Meadow, CA	MK284957
H31_EML06	<i>Bufo canorus</i>	Emmigrant Meadow, CA	MK284958
H32_EML10	<i>Bufo canorus</i>	Emmigrant Meadow, CA	MK284959
H33_EML11	<i>Bufo canorus</i>	Emmigrant Meadow, CA	MK284960
H34_EML19	<i>Bufo canorus</i>	Emmigrant Meadow, CA	MK284961
H35_ET100	<i>Bufo boreas</i>	Elliot Reserve, CA	MK284962
H36_ET101	<i>Bufo boreas</i>	Elliot Reserve, CA	MK284963
H37_GR2	<i>Bufo boreas</i>	Granite Range, NV	MK284964
H38_GR3	<i>Bufo boreas</i>	Granite Range, NV	MK284965
H39_GR7	<i>Bufo boreas</i>	Granite Range, NV	MK284966
H40_GR8	<i>Bufo boreas</i>	Granite Range, NV	MK284967
H41_HC50	<i>Bufo monfontanus</i>	Hot Creek Canyon, NV	MK284968
H47_MC2	<i>Bufo boreas</i>	Mud Creek, OR	MK284969
H48_MC3	<i>Bufo boreas</i>	Mud Creek, OR	MK284970
H49_MC8	<i>Bufo boreas</i>	Mud Creek, OR	MK284971
H50_MK1	<i>Bufo boreas</i>	Mary's Creek, NV	MK284972
H51_MK10	<i>Bufo boreas</i>	Mary's Creek, NV	MK284973
H52_MK22	<i>Bufo boreas</i>	Mary's Creek, NV	MK284974
H53_MK25	<i>Bufo boreas</i>	Mary's Creek, NV	MK284975
H54_MR1	<i>Bufo boreas</i>	Mojave River, NV	MK284976
H55_MR4	<i>Bufo boreas</i>	Mojave River, NV	MK284977
H56_NV2	<i>Bufo boreas</i>	Newark Valley, NV	MK284978
H57_OL11	<i>Bufo boreas</i>	Owens Dry Lake, CA	MK284979
H58_OS5	<i>Bufo boreas</i>	Orchard Spring, NV	MK284980
H59_PC3	<i>Bufo boreas</i>	Peavine Creek, NV	MK284981
H60_PF1	<i>Bufo boreas</i>	Pine Forest Range, NV	MK284982
H61_PV1	<i>Bufo boreas</i>	Palamino Valley, NV	MK284983
H62_PV4	<i>Bufo boreas</i>	Palamino Valley, NV	MK284984
H63_RS2	<i>Bufo boreas</i>	Rock Springs, NV	MK284985
H64_RS3	<i>Bufo boreas</i>	Rock Springs, NV	MK284986
H65_RV50	<i>Bufo nevadensis</i>	Railroad Valley, NV	MK284987
H66_RV51	<i>Bufo nevadensis</i>	Railroad Valley, NV	MK284988
H67_SL10	<i>Bufo boreas</i>	Swan Lake, NV	MK284989
H68_SL15	<i>Bufo boreas</i>	Swan Lake, NV	MK284990

**Table 3.** Continued.

Haplotype code	Taxon	Locality	GenBank accession numbers for CR1600 ( <i>n</i> = 62)
H69_SL16	<i>Bufo boreas</i>	Swan Lake, NV	MK284991
H70_SL24	<i>Bufo boreas</i>	Swan Lake, NV	MK284992
H71_SL9	<i>Bufo boreas</i>	Swan Lake, NV	MK284993
H72_WL13	<i>Bufo boreas</i>	Walker Lake, NV	MK284994
<i>boreas</i> .KaUT	<i>Bufo boreas</i>	Kane Co., UT	EF532065
	<i>Bufo boreas</i>	Kane Co., UT	EF532066
	<i>Bufo boreas</i>	Kane Co., UT	EF532067
<i>boreas</i> .BeUT	<i>Bufo boreas</i>	Box Elder Co., UT	EF532075
	<i>Bufo boreas</i>	Box Elder Co., UT	EF532076
<i>boreas</i> .SuUT	<i>Bufo boreas</i>	Summit Co., UT	EF532082
<i>boreas</i> .LaCO	<i>Bufo boreas</i>	Larimer Co., CO	EF532092
<i>boreas</i> .LaCO2	<i>Bufo boreas</i>	Larimer Co., CO	EF532094
<i>boreas</i> .LaCO3	<i>Bufo boreas</i>	Larimer Co., CO	EF532084
<i>boreas</i> .GuCO	<i>Bufo boreas</i>	Gunnison Co., CO	EF532089
<i>boreas</i> .SuCO	<i>Bufo boreas</i>	Summit Co., CO	EF532086
<i>boreas</i> .CHCO	<i>Bufo boreas</i>	Chafee Co., CO	EF532085
<i>boreas</i> .CHCO2	<i>Bufo boreas</i>	Chafee Co., CO	EF532088
<i>boreas</i> .CCCO	<i>Bufo boreas</i>	Clear Creek Co., CO	EF532095
<i>boreas</i> .CCCO2	<i>Bufo boreas</i>	Clear Creek Co., CO	EF532098
<i>boreas</i> .CCCO3	<i>Bufo boreas</i>	Clear Creek Co., CO	EF532097
<i>boreas</i> .MiCO	<i>Bufo boreas</i>	Mineral Co., CO	EF532087

**Table 4.** Table of least squares means generated from regressions of MANCOVA analyses for SVL and 13 size corrected traits (see Materials and Methods) against SVL for each species examined within the *B. boreas* species complex. Each value includes upper and lower 95% confidence intervals (CI). Bolded values indicate statistically significant different states in pairwise comparison identified in Tukey HSD *post hoc* tests ( $P < 0.05$ ) with larger (↑) and smaller character states (↓) identified.

	<i>B. nevadensis</i> ( <i>n</i> = 50)	<i>B. monfontanus</i> ( <i>n</i> = 42)	<i>B. boreas</i> ( <i>n</i> = 289)	<i>B. nelsoni</i> ( <i>n</i> = 31)	<i>B. exsul</i> ( <i>n</i> = 30)	<i>B. williamsi</i> ( <i>n</i> = 76)
SVL	<b>66.3↓</b>	<b>61.6↓</b>	<b>82.3↑</b>	<b>80.8↑</b>	<b>64.0↓</b>	<b>56.3↓</b>
CI	62.4, 70.1	57.6, 65.5	81.0, 83.6	77.0, 84.7	60.1, 67.9	52.4, 60.2
HL	<b>22.6↑</b>	<b>21.3↓</b>	<b>22.7↑</b>	<b>22.9↑</b>	<b>21.5↓</b>	<b>21.7↓</b>
CI	22.2, 23.0	20.9, 21.8	22.6, 22.8	22.6, 23.4	21.1, 21.9	21.1, 21.9
HW	25.3	25.5	25.9	<b>26.8↑</b>	<b>24.4↓</b>	<b>24.5↓</b>
CI	24.9, 25.8	25.0, 26.0	25.8, 26.1	26.4, 27.3	23.9, 24.9	24.0, 25.1
SL	<b>4.74↓</b>	<b>5.29↑</b>	<b>5.31↑</b>	<b>5.22↑</b>	<b>5.00↓</b>	<b>5.52↑</b>
CI	4.56, 4.92	5.10, 5.48	5.24, 5.37	5.05, 5.40	4.82, 5.19	5.32, 5.72
IND	4.99	4.84	4.78	<b>5.09↑</b>	4.74	4.79
CI	4.82, 5.15	4.66, 5.02	4.72, 4.83	4.92, 5.25	4.57, 4.91	4.61, 4.97
ED	<b>7.23↓</b>	<b>6.91↓</b>	<b>7.11↓</b>	7.33	<b>6.85↓</b>	<b>7.65↑</b>
CI	7.03, 7.42	6.70, 7.12	7.05, 7.18	7.13, 7.52	6.65, 7.05	7.44, 7.87
IOD	11.8	<b>12.4↑</b>	<b>12.3↑</b>	<b>11.7↓</b>	<b>11.2↓</b>	<b>11.6↓</b>
CI	11.5, 12.2	12.1, 12.7	12.2, 12.4	11.4, 12.0	10.8, 11.5	11.2, 12.0
TYM	<b>3.99↓</b>	<b>3.97↓</b>	<b>3.99↓</b>	<b>3.95↓</b>	<b>3.95↓</b>	<b>4.35↑</b>
CI	1.5–3.8	3.79, 4.14	3.93, 4.04	3.79, 4.11	3.78, 4.11	4.17, 4.53
PW	<b>5.47↓</b>	6.70	<b>6.75↑</b>	6.62	<b>6.18↓</b>	6.50
CI	5.20, 5.75	6.40, 7.00	6.65, 6.84	6.36, 6.89	5.89, 6.46	6.20, 6.81
PL	<b>7.86↓</b>	<b>9.62↑</b>	<b>9.52↑</b>	<b>8.49↓</b>	<b>7.86↓</b>	<b>8.39↓</b>
CI	7.47, 8.24	9.20, 10.03	9.39, 9.66	8.11, 8.87	7.47, 8.26	7.97, 8.82
IPD	14.9	<b>13.9↓</b>	<b>14.9↑</b>	14.8	<b>14.1↓</b>	14.5
CI	14.4, 15.3	13.4, 14.3	14.7, 15.0	14.5, 15.2	13.7, 14.5	14.1, 15.0
FL	<b>30.3↑</b>	<b>26.1↓</b>	<b>31.0↑</b>	29.8	<b>28.6↓</b>	<b>28.8↓</b>
CI	29.7, 30.9	25.5, 26.8	30.7, 31.2	29.2, 30.4	28.0, 29.3	28.1, 29.5
TL	<b>29.6↑</b>	<b>27.5↓</b>	<b>30.3↑</b>	28.9	28.4	<b>27.6↓</b>
CI	29.0, 30.2	26.9, 28.1	30.1, 30.6	28.3, 29.5	27.8, 29.0	26.9, 28.3
FTL	<b>31.6↑</b>	<b>29.8↓</b>	<b>32.0↑</b>	31.2	30.2	<b>29.1↓</b>
CI	30.8, 32.4	28.9, 30.6	31.8, 32.3	30.5, 32.0	29.3, 31.0	28.9, 30.6



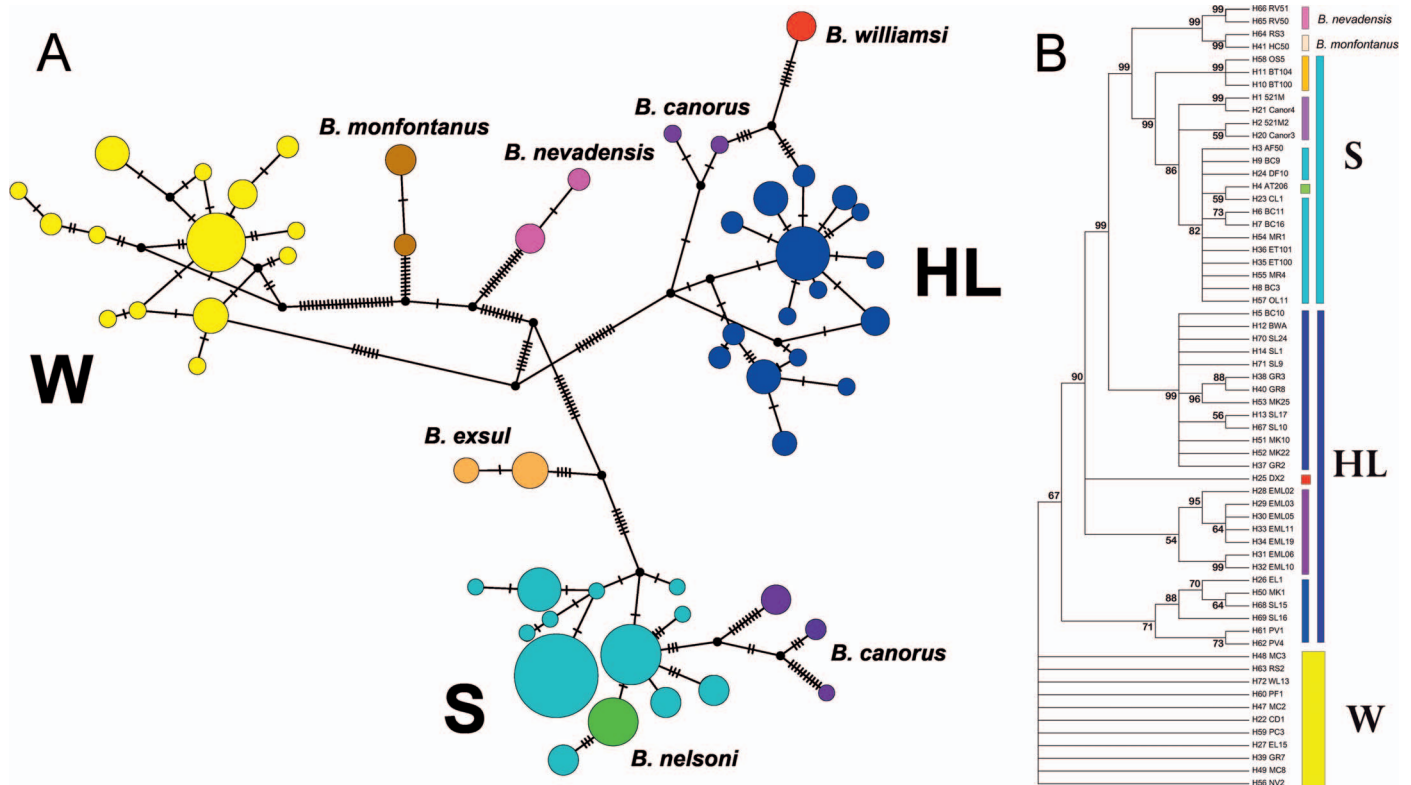


**Fig. 3.** Molecular examination of *B. boreas* species complex. (A) The TCS haplotype network was constructed using 257 sequences (1,622 bp) obtained from toad sampling (Fig. 1B) resulting in 62 unique haplotypes. Circle sizes correspond with the number of individuals of a particular haplotype. Major haplotype clades identified within *B. boreas* (W—Western Great Basin [yellow], HL—Humboldt-Lahontan [blue], and S—Mojave [aqua]) and to localized species (*B. canorus* [purple], *B. exsul* [tan], *B. nelsoni* [orange], *B. williamsi* [red]) and highlight the genetic divergence of both *B. nevadensis* (mauve) and *B. monfontanus* (brown). (B) Maximum likelihood tree derived from the control region of mitochondrial genome. Branches corresponding to partitions reproduced in less than 50% bootstrap replicates are collapsed. The percentage of replicate trees in which the associated taxa clustered together in the bootstrap test (500 replicates) are shown next to the branches (Felsenstein, 1985). See Data Accessibility for tree file.

appear to be polyphyletic or paraphyletic with lineages that occur in the Humboldt-Lahontan and Mojave clades, a result consistent with previous studies (Graybeal, 1993; Goebel, 1996; Shaffer et al., 2000; Stephens, 2001; Goebel et al., 2009; Switzer et al., 2009; Gordon et al., 2017).

Assessment of nucleotide diversity evaluating genetic distances for both *B. nevadensis*, new species, and *B. monfontanus*, new species, uncovered higher percentages of differentiation than other congeneric taxa within the *B. boreas* species complex (Table 5). *Bufo nevadensis*, new species, average genetic distance compared to *B. boreas* is 3.5% and *B. monfontanus* new species is 3.2%, and despite their seemingly close relative proximity (Figs. 1, 5B), these two species are highly differentiated from each other at 2.0% divergence (Table 5).

Comparing *Bufo nevadensis*, new species, and *B. monfontanus*, new species, to populations of *B. boreas* outside of the Great Basin, we used maximum likelihood to test evolutionary hypotheses which yielded support for the new species' divergence and illustrates close ancestry with populations of *B. boreas* in Utah and Colorado (Fig. 4). *Bufo nevadensis*, new species, forms a terminal clade and is basal to populations of boreal toads near the northwestern Utah border and Colorado (Table 3, Fig. 4), and genetic distance of this species to *B. boreas* was 1.7%. *Bufo monfontanus*, new species, forms a terminal end and represents a divergent lineage, but shares a haplotype for this marker with one boreal toad from the

northwestern corner of Utah in Box Elder County (Fig. 4) with an average genetic distance of 1.3%. Additional molecular markers may provide greater insight into the fine-scale relationships of these newly described species and taxa of the *B. boreas* species complex.

#### ***Bufo (Anaxyrus) nevadensis*, new species**

urn:lsid:zoobank.org:act:D9F8FACC-74DB-4D01-84AE-07CCB9400188

Railroad Valley Toad

Figures 1–4, 5B, 6; Tables 1, 4–5

**Holotype.**—CAS 259272, adult female (Fig. 6, Table 1), United States, Nevada, Nye County, Railroad Valley, Locke's Preserve, 38°33'9.1"N, 115°46'12.8"W, M. R. Gordon, 5 May 2015.

**Paratypes.**—UNR 7905, adult male; UNR 7906, adult female; UNR 7907, adult female; UNR 7908, adult male; UNR 7909, adult female; all individuals collected within the identified home range in Railroad Valley, 38°33'9.1"N, 115°46'12.8"W, M. R. Gordon, K. Guadalupe, and C. Burg, 5 May 2015 (Fig. 5B).

**Diagnosis.**—*Bufo (Anaxyrus) nevadensis* is a member of the Great Basin *B. boreas* species complex (Blair, 1972), but traditionally has been identified as *B. boreas* due to its occurrence within the Western Toad's geographic range, yet

**Table 5.** Estimates of evolutionary divergence between mitochondrial DNA control region sequences from taxa of the *B. boreas* species complex within the Great Basin. The number of base substitutions per site from between sequences is shown. Analyses were conducted using Jukes-Cantor model (Jukes and Cantor, 1969), which involved 14 nucleotide sequences (Fig. 1B), in Mega7 (Kumar et al., 2016). All positions containing gaps and missing data were eliminated, which resulted in a final dataset of 1429 positions. Pairwise comparisons against congeners of the *B. boreas* species complex for *B. nevadensis* and *B. monfontanus* are indicated in bold.

<i>B. canorus</i> (S)													
<i>B. nelsoni</i>	0.011												
<i>B. exsul</i>	0.011	0.010											
<i>B. boreas</i> (CA)	0.030	0.031	0.027										
<i>B. williamsi</i>	0.031	0.030	0.027	0.018									
<i>B. canorus</i> (N)	0.032	0.030	0.029	0.018	0.010								
<i>B. b. halophilus</i>	0.013	0.006	0.011	0.031	0.031	0.031							
<b><i>B. monfontanus</i></b>	<b>0.030</b>	<b>0.032</b>	<b>0.029</b>	<b>0.032</b>	<b>0.029</b>	<b>0.034</b>	<b>0.034</b>						
<i>B. boreas</i> (OR)	0.028	0.029	0.024	0.004	0.016	0.016	0.029	<b>0.031</b>					
<i>B. boreas</i> (NV)	0.031	0.030	0.027	0.018	0.010	0.008	0.031	<b>0.032</b>	0.016				
<b><i>B. nevadensis</i> 1</b>	<b>0.030</b>	<b>0.032</b>	<b>0.029</b>	<b>0.035</b>	<b>0.032</b>	<b>0.037</b>	<b>0.032</b>	<b>0.020</b>	<b>0.034</b>	<b>0.037</b>			
<b><i>B. nevadensis</i> 2</b>	<b>0.031</b>	<b>0.033</b>	<b>0.030</b>	<b>0.036</b>	<b>0.033</b>	<b>0.037</b>	<b>0.033</b>	<b>0.021</b>	<b>0.034</b>	<b>0.037</b>	0.001		
<i>B. punctatus</i>	0.184	0.185	0.184	0.185	0.190	0.186	0.184	0.187	0.183	0.188	0.188	0.189	
<i>B. punctatus</i>	0.188	0.189	0.188	0.189	0.195	0.190	0.188	0.194	0.187	0.191	0.195	0.196	0.012

is distinct from *B. boreas* by a combination of morphological characters (Figs. 2, 6, Tables 1, 4), genetic evidence (Figs. 3, 4, Table 5), and restricted geographic distribution (Fig. 5B). *Bufo nevadensis* is distinguished from *B. boreas* due to its small adult body size (SVL is approximately 2 cm smaller than *B. boreas*; Tables 1, 4); significantly, but modestly longer head with a relatively shorter snout; well-separated, perceptibly short and narrow parotoid glands; significantly, but comparatively long legs, large hind feet (Fig. 6B); and distinctive mottling of venter (Fig. 6B, D).

*Bufo nevadensis* is among the smallest terrestrial bufonids within the *B. boreas* species complex (Tables 1, 4). However, this new species exhibits a relatively large head unlike similarly small toads, *B. exsul* and *B. monfontanus*, new species, with a significantly, but comparatively shorter snout distinctive from all species within the complex except *B. exsul* (Table 4). The well-separated and severely reduced parotoid glands exhibited in *B. nevadensis* is divergent from all taxa within the *B. boreas* species complex, and the shortened gland length distinguishes *B. nevadensis* from both *B. boreas* and *B. monfontanus*, new species. *Bufo nevadensis* has statistically significant, relatively long legs; longer femur than exhibited in *B. exsul*, *B. monfontanus*, new species, and *B. williamsi*, and a longer tibia and hind feet, which separate *B. nevadensis* from *B. monfontanus*, new species, and *B. williamsi* (Table 4). In addition to morphological shape differences, *B. nevadensis* displays a dominantly brown and gray toned dorsum with prominent warts and heavily creased skin, which differs from *B. exsul*, *B. monfontanus*, new species, *B. nelsoni*, and *B. williamsi*. The venter of *B. nevadensis* is similar to *B. exsul* and *B. williamsi*, exhibiting black mottling contrasted against a white background color on the anterior sides of the limbs and belly. The presence of a dorsal stripe is extremely variable among individuals of *B. nevadensis*, as is similar to the other members of the *B. boreas* species complex, with the exception of *B. exsul*. Small, irregular tibial glands may be present in individuals, but this characteristic is highly variable.

In mature male *B. nevadensis*, distinct nuptial pads develop on the dorsal side of the first finger, a typical secondary sexual characteristic exhibited among most bufonids. This species lacks an advertisement call, but it emits a release call

when males come in contact with one another which sound like the weeping of a chick and is similar among congeners of the *B. boreas* complex (Stebbins, 2003).

**Description of holotype.**—Body relatively small and robust (SVL = 62.5 mm); head wider (HW = 20.1 mm) than long (HL = 17.2 mm; 85% head length to head width). Snout subelliptical in dorsal view; snout profile moderately truncate in lateral view (SL = 7.5 mm; 1.5 times longer than eye diameter). Canthus rostralis distinct and cuneate. Loreal region slightly concave. Nostrils slightly protuberant, directed dorsolaterally, and closer to anterior corner of eye than to snout. Internarial distance (IND = 3.8 mm) 75% of interorbital distance (IOD = 4.8 mm). Eyes well separated; interorbital space nearly equivalent to eye diameter (ED = 4.8 mm). Upper eyelids prominent in dorsal view; eyes slightly breach profile margin. Tympanum (TYM = 3.0 mm) distinct, subovoid, relatively small (52% of eye diameter). Supratympanic fold present. Parotoid glands weakly present viewed above; parotoid glands narrow (PW = 3.7 mm), severely tapered at posterior corner of eye in lateral view. Parotoid glands 1.5 times longer (PL = 7.5 mm) than eye diameter; parallel, well separated (IPD = 12.3 mm). Forearms robust. Fingers unwebbed; relative length III > I > II > IV; tips rounded, subarticular tubercles moderate, accessory palmar tubercles small, round. Inner metacarpal tubercle distinct, round. Palmar tubercle prominent, elliptical. Hind limbs long; femur slightly longer (FL = 21.2 mm) than tibia (TL = 18.7 mm). Tibial glands irregular, scarcely defined, half the length of parotoid gland. Tarsal fold present; hind feet webbed proximally (FTL = 37.0 mm). Relative toe lengths IV > III > V > II > I; toe tips rounded. Subarticular tubercles faintly evident, small, round. Plantar tubercles numerous, small. Inner metatarsal tubercle pronounced, elevated, relatively large, elliptical. Outer metatarsal tubercle distinct, ovoid. Skin warty on dorsum; primary warts elevated, irregular; finely granular skin between elevated warts from interorbital space increasing in coarseness toward posterior margin of dorsum at articulation with femur. Hind limbs warty; tubercles small, moderate. Venter coarse, seat patch conspicuous.

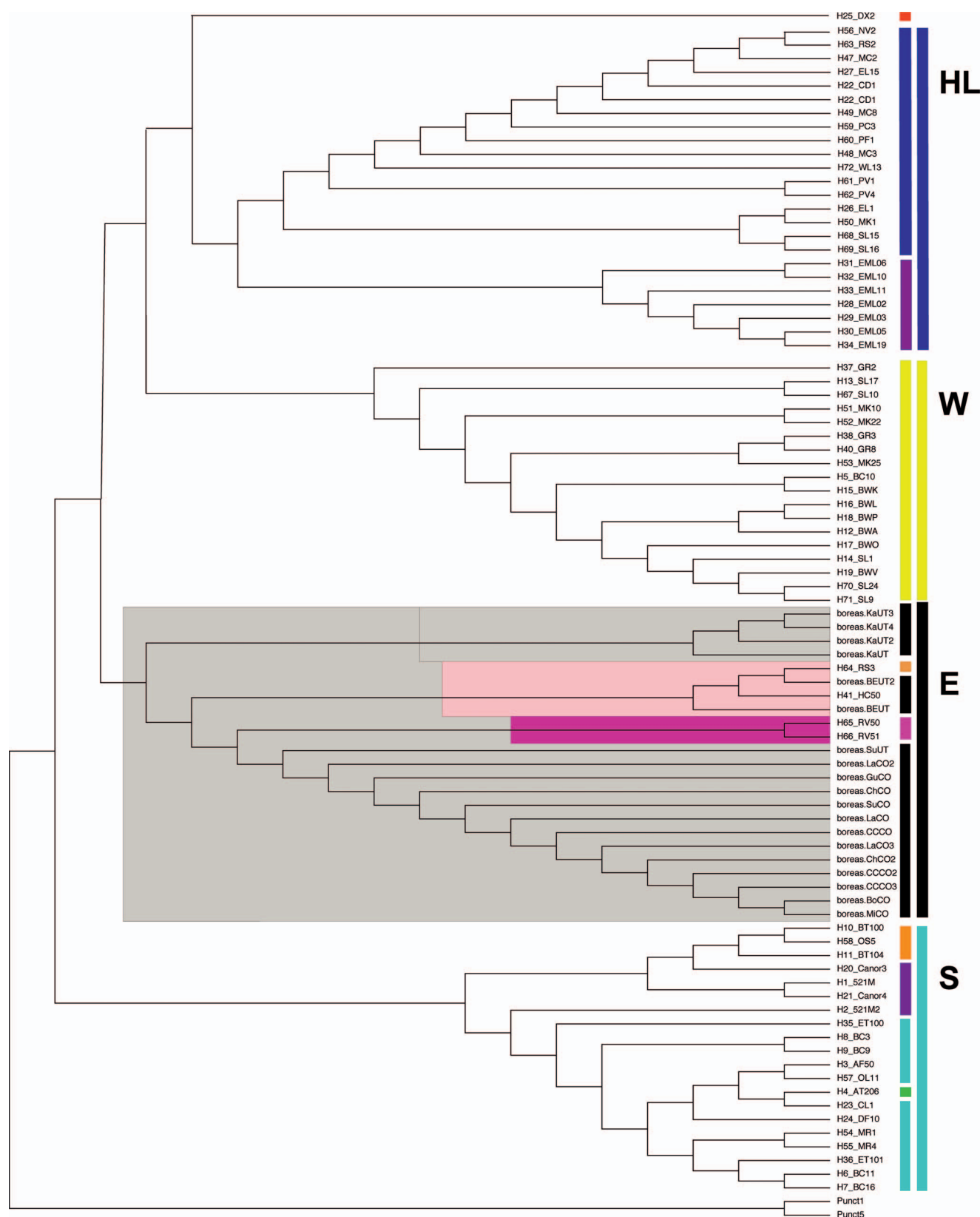


**Fig. 4.** Molecular phylogenetic reconstruction of region-wide *B. boreas* species complex diversity. Tree reconstruction included sequence data (Table 3) from *B. boreas* outside the Great Basin to evaluate the relationships between toads from Hot Creek and Railroad Valley and Utah and Colorado toads using the maximum likelihood method. Minor and major groups identified. Terminal ends include haplotype number and locality of collection. Sequences of *B. boreas* from outside the Great Basin (Table 3) include this taxon name within terminal end identifier. Minor groups include localized species within the Great Basin: *B. nelsoni* (green), *B. exsul* (orange), *B. canorus* (purple), *B. williamsi* (red), and newly delimited species, *B. monfontanus* (mauve) and *B. nevadensis* (pink), of the major group identified as the Eastern Great Basin clade (black bar). Two haplotypes of the root are shown. See Data Accessibility for tree file.



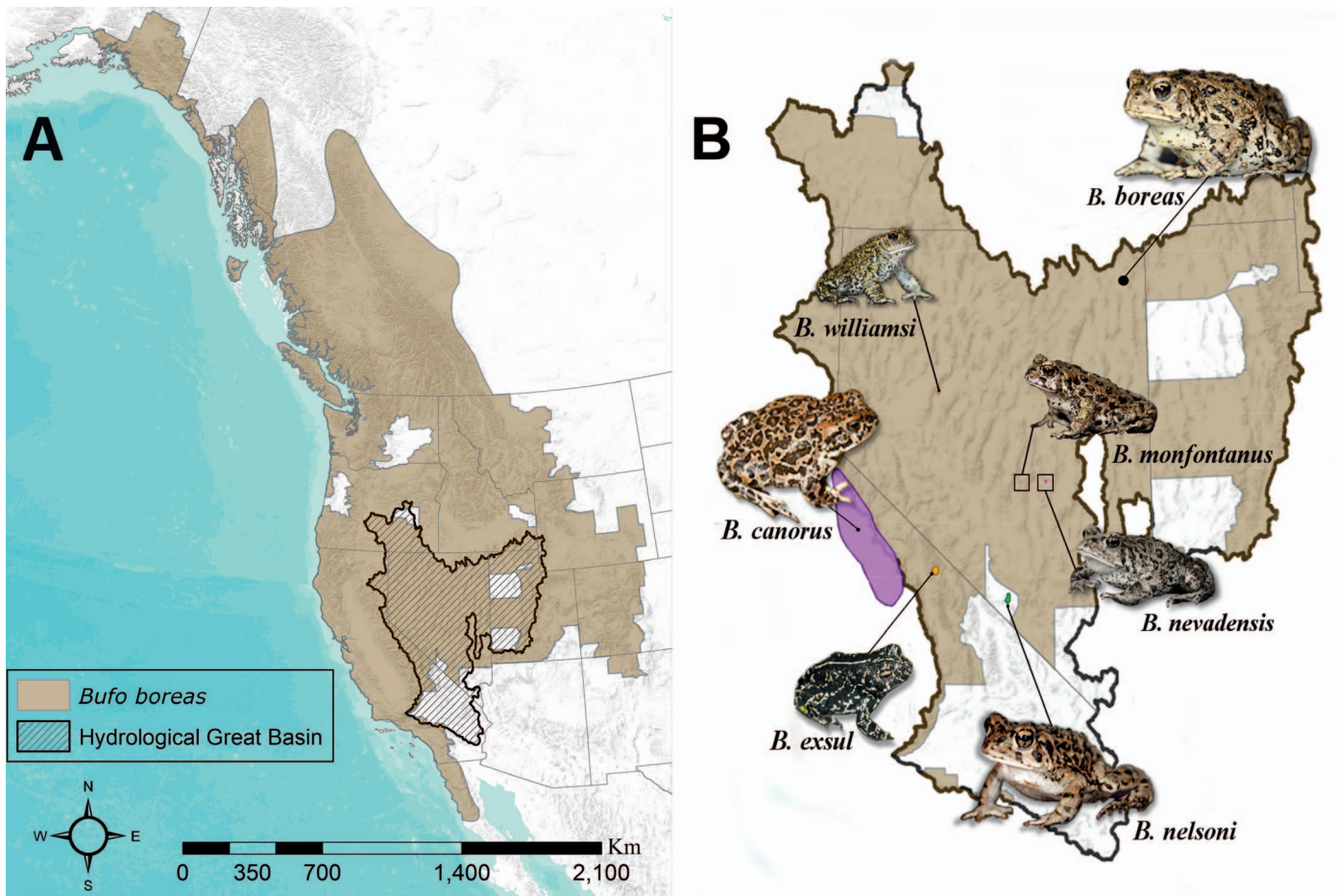


**Fig. 5.** Distribution of *B. boreas* and Great Basin *B. boreas* species complex. (A) The range-wide distribution of *Bufo boreas* shown in brown with hydrologic Great Basin outlined in black and hash mark interior within the western United States (Gordon et al., 2017). (B) *Bufo boreas* species complex and new species shown within hydrologic Great Basin, illustrating the small ranges of localized endemics. Spatial data for all toads except *B. williamsi*, *B. nevadensis*, and *B. monfontanus* provided by IUCN (2015). Images taken by M. R. Gordon except *B. canorus*, with photo credit to G. Nafis.

**Color in life.**—Dorsal ground color of holotype light brownish gray, flecked with dark brown, irregular spotting (Fig. 6A). Grayish head dappled with dark brown patches, upper eyelids finely speckled black. Smooth dark olive brown blotches along prefrontal to frontal area of head and interorbital space. Pupil black, horizontal with gold streaked iris. Brownish gray parotoid glands exhibit minor black to dark brown spotting. Cream colored dorsal stripe present, originating posteriorly at nares and terminating at posterior margin of urostyle. Elevated, dark olive brown warts at interparotoid space, along dorsum; some warts set in black blotches; olive streaking connects warts along midline bordering dorsal strip; dorsolaterally, olive to dark brown wart color streaked against brownish gray background color. At midaxillary line, black streaking contrasts against white background. Throat white with minor black spotting near lower lip. Venter mottled black against white background color (Fig. 6B). In dorsal view, forelimbs have minor dark olive banding and olive patches against light grayish brown ground color; hind limbs exhibit dark olive brown banding and patches against light grayish brown ground color down to heavily dappled olive feet atop brownish gray background color. Along medial and ventral sides of hind limbs, black

spotting and patches occur against white ground color down to medial edge of feet, which appear dark gray on underside.

**Variation.**—In paratypes, background color ranges from light gray to light brownish gray; warts may be olive colored to olive brown and may be set in black blotches. Brown to dark brown spotting around front of head; minor black spotting on throat and minor to heavy black mottling occur on venter.

**Color in preservative.**—Color is similar to that in life (Fig. 6A, B) with some notable differences. Overall background color in the holotype appears gray (Fig. 6C). Along dorsum, dark brown warts flattened and appear as heavy streaks against brownish gray background adjacent to dorsal stripe. Marbling along midaxillary line and venter less vibrant than in life and appear dark gray against white ground color and seat patch muted light gray (Fig. 6D).

**Distribution.**—*Bufo nevadensis* is known only to occur near and within the spring-fed wetland areas of Lockes Ranch (1,460 m above sea level), a protected wildlife management area located in Railroad Valley, an east-central desert basin between the Pancake Range and Grand Range of Nye County, Nevada (Fig. 5B). The critical marshland habitat for this endemic toad is



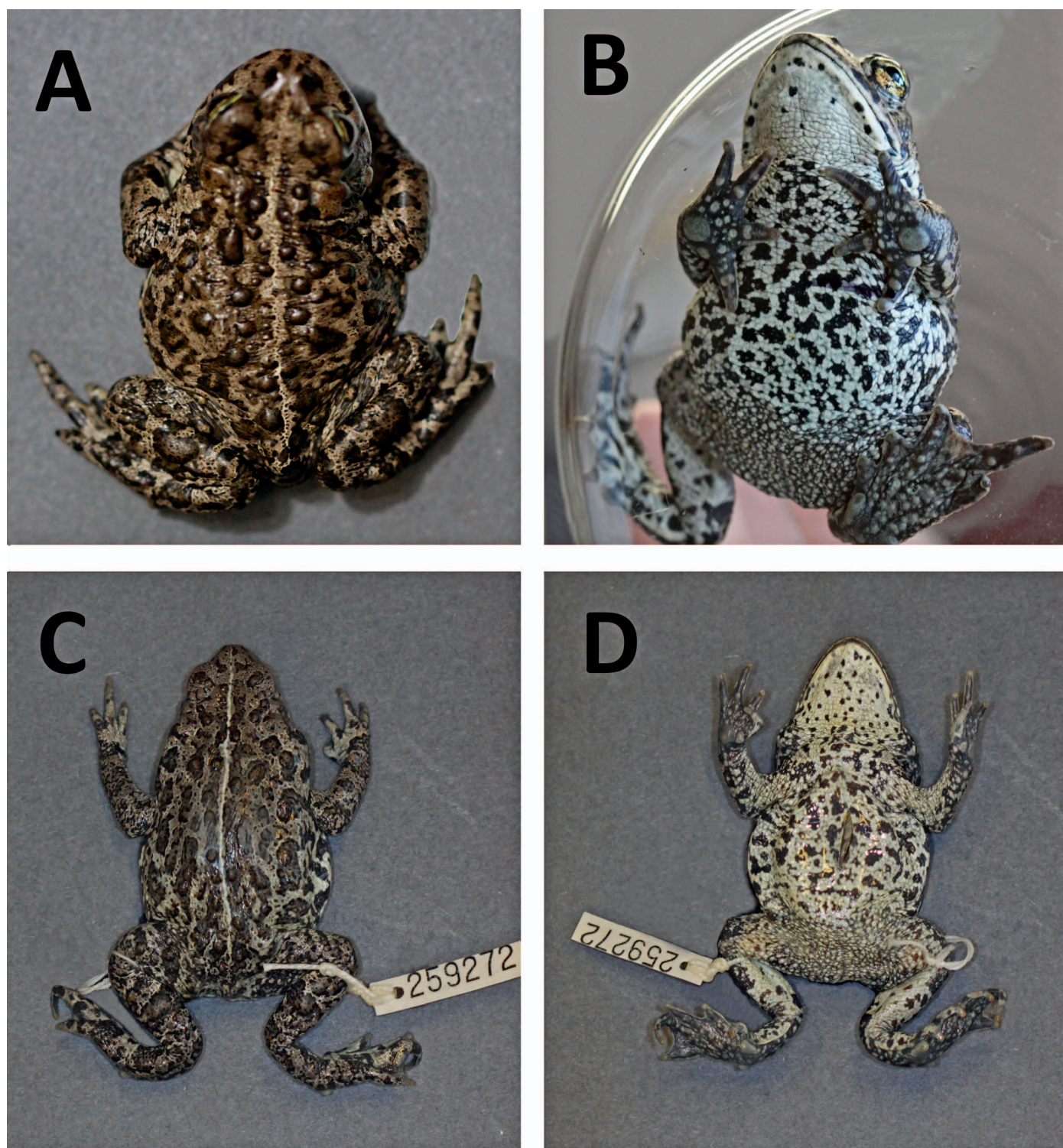


**Fig. 6.** Photographs of *Bufo (Anaxyrus) nevadensis*, new species, holotype (CAS 259272). Female toad in life: (A) dorsal view and (B) ventral view; and in preservative: (C) dorsal view and (D) ventral view. Photographs taken by M. R. Gordon.

solely fed from Big, Reynolds, and Hay Corral springs which results in a severely restricted range with an estimated distribution of 1.8 km<sup>2</sup>. These outflows are remote and isolated, surrounded by cold desert habitat dominated by Big Sagebrush (*Artemisia tridentata* ssp. *tridentata*), Greasewood (*Sarcobatus vermiculatus*), Rubber Rabbitbrush (*Ericameria nauseosa*), and saltbush (*Atriplex* spp.) with limited usable corridors for amphibian dispersal, which likely restricts this

species' movement to other spring localities within Railroad Valley. *Bufo nevadensis* co-occurs with the federally listed threatened Railroad Valley Springfish, *Crenichthys nevadae*, and the Great Basin Spadefoot, *Spea intermontana*.

**Life history and behavior.**—*Bufo nevadensis* is nocturnal, emerging at dusk, and can be found in shallow water or among the vegetation in the perimeter band that transitions



from riparian to sagebrush steppe habitat. Characteristic of cold deserts, Railroad Valley experiences extreme fluctuations in day and nighttime temperatures as well as season-to-season variation. As is common for other members of the *B. boreas* complex, these toads likely retreat to burrows in the fall, not emerging until spring, when males begin to congregate in shallow water for breeding. Mature males, similar to other members of the *B. boreas* complex (with the singular exception of *B. canorus*), do not have an advertisement call, but emit a release call when males come in close contact with one another. Egg masses and tadpoles develop in still, shallow water amid the marshy vegetation of the wetland habitat.

The population size for this species is unknown; however, the extreme isolation and restricted range may indicate that the population numbers may be small. Little is known regarding the dispersal and non-breeding behavior of this rare toad.

**Etymology.**—The species name is a derivative from the state of Nevada (U.S.A) where this rare toad occurs and pays homage to the unique biodiversity found in the desert landscape of its home state.

**Remarks.**—Railroad Valley is a geothermally active area within the Range and Basin Province with significant opportunities for anthropogenic energy production, including extraction of its oil reservoirs (Liu et al., 1997) that continue to contribute to ongoing economic interests in the valley which are currently overseen by the Bureau of Land Management. Discovery of this rare new species should elicit high conservation concerns due to its severely restricted range and limitations to dispersal due to isolation and remoteness of the spring-fed habitat upon which *B. nevadensis* is dependent. Any further human anthropogenic modifications of habitat that may degrade this extremely important habitat would imperil this toad. However, with new species designation, conservation initiatives would provide a platform for ongoing policy and monitoring to allow this this endemic toad to persist.

***Bufo (Anaxyrus) monfontanus*, new species**

urn:lsid:zoobank.org:act:58EA3AB0-7EF3-4CF3-B832-

5938DF05021C

Hot Creek Toad

Figures 1–4, 5B, 7; Tables 1, 4–5

**Holotype.**—CAS 259273, adult male (Fig. 7, Tables 1, 4), United States, Nevada, Nye County, Hot Creek Canyon, 38°32′19.32″N, 116°27′32.9″W, M. R. Gordon, 6 May 2015.

**Paratypes.**—UNR 7910, adult male; UNR 7911, adult male; UNR 7912, adult male; UNR 7913, adult male; UNR 7914, adult male; UNR 7915, adult male; UNR 7916, adult male; UNR 7917, adult male; all individuals collected within the identified home range, Hot Creek Canyon, 38°32′19.32″N, 116°27′32.9″W (Fig. 5B), M. R. Gordon, 6 May 2015.

**Diagnosis.**—*Bufo (Anaxyrus) monfontanus* occurs within the range of *B. boreas* but is distinct from the Western Toad by a combination of diagnostic morphological characters (Figs. 2, 7, Tables 1, 4), genetic evidence (Fig. 3, Table 5), and restricted geographic distribution (Fig. 5B). *Bufo monfontanus* is distinguishable from *B. boreas* by having a small adult body

size (SVL is 2 cm smaller than *B. boreas*; Tables 1, 5); significantly, but modestly shorter head; perceptibly large, parotoid glands; significantly, but comparatively shorter legs with small hind feet; and weakly warted body (Fig. 7A).

*Bufo monfontanus* is among the smallest bufonids within the *B. boreas* species complex, and it is only larger than *B. williamsi* (Tables 1, 4). *Bufo monfontanus* has a significant, but relatively shorter head with a comparatively long snout, with a relative head width more comparable to larger-sized taxa *B. boreas* and *B. nelsoni* (Table 4). An important diagnostic feature among *B. monfontanus* is the presentation of well-defined, relatively large parotoid glands, which distinguishes this small toad from all other small-sized toads within the *B. boreas* species complex (Table 4). *Bufo monfontanus* has shorter legs; significantly, but relatively the shortest femur and tibia of all taxa within the *B. boreas* species complex and relatively small feet distinct from both *B. boreas* and *B. nevadensis* (Table 4). The dorsal stripe is extremely variable among individuals of *B. monfontanus*; a characteristic typical among taxa within the *B. boreas* species complex with the exception of *B. exsul*. Small, irregular tibial glands may be present among individuals of *B. monfontanus* as seen in both *B. nevadensis* and *B. williamsi*.

In adult male *B. monfontanus*, distinct nuptial pads develop on the dorsal side of the first finger which is a typical secondary sexual characteristic exhibited among most bufonids. Akin to congeners of the *B. boreas* species complex, except *B. canorus*, males of this species emit a release call that sounds like a weeping chick (Stebbins, 2003).

**Description of holotype.**—Body small, robust (SVL = 59.6 mm); head wider (HW = 19.3 mm) than long (HL = 16.2 mm). Snout subovoid in dorsal view; snout rounded in lateral view, long (SL = 6.4 mm; 40% of head length). Canthus rostralis distinct, concave, angular, sloping up to medial orbital margins. Loreal region slightly concave. Nostrils protuberant, directed dorsolaterally, closer to anterior corner of eye than end of snout. Internarial distance 75% of eye-to-naris distance (IND = 2.3 mm). Relatively moderate eyes well separated (ED = 4.4 mm; IOD = 3.8 mm); eyes do not breach snout profile in dorsal view. Tympanum distinct, oval, small (TYM = 2.5 mm; 53% of eye diameter). Supratympanic fold weakly present, flat. Parotoid glands longer (PL = 8.8 mm) than wide (PW = 5.3 mm; length nearly twice eye diameter). Glands elevated, slightly convergent at posterior ends in dorsal view. In lateral view, parotoid glands elongated longitudinally from posterior corner of eye, oval, wider than the eye (1.4 times eye diameter). Interparotoid space large (IPD = 9.4 mm; 2.5 times interorbital distance). Forearms robust, smooth. Fingers unwebbed; relative lengths III > I > IV > II; nuptial pads present, raised on dorsal side of digit I; tips rounded, subarticular tubercles moderate, round; accessory palmar tubercles small, round. Inner metacarpal tubercle raised, prominent, round. Palmar tubercle distinct, large, subovoid, borders medial margin of inner metacarpal tubercle. Hind limbs long; femur longer (FL = 23.1 mm) than tibia (TL = 19.7 mm). Tibial gland weakly present in dorsal view and equivalent to the width of the parotoid gland. Tarsal fold present. Hind feet webbed proximally (FTL = 35.0 mm). Relative toe lengths IV > III > V > II > I; tips rounded. Subarticular tubercles distinct, small and round; plantar tubercles numerous, small. Inner metatarsal tubercle conspicuous, elevated, relatively large and elliptical. Outer



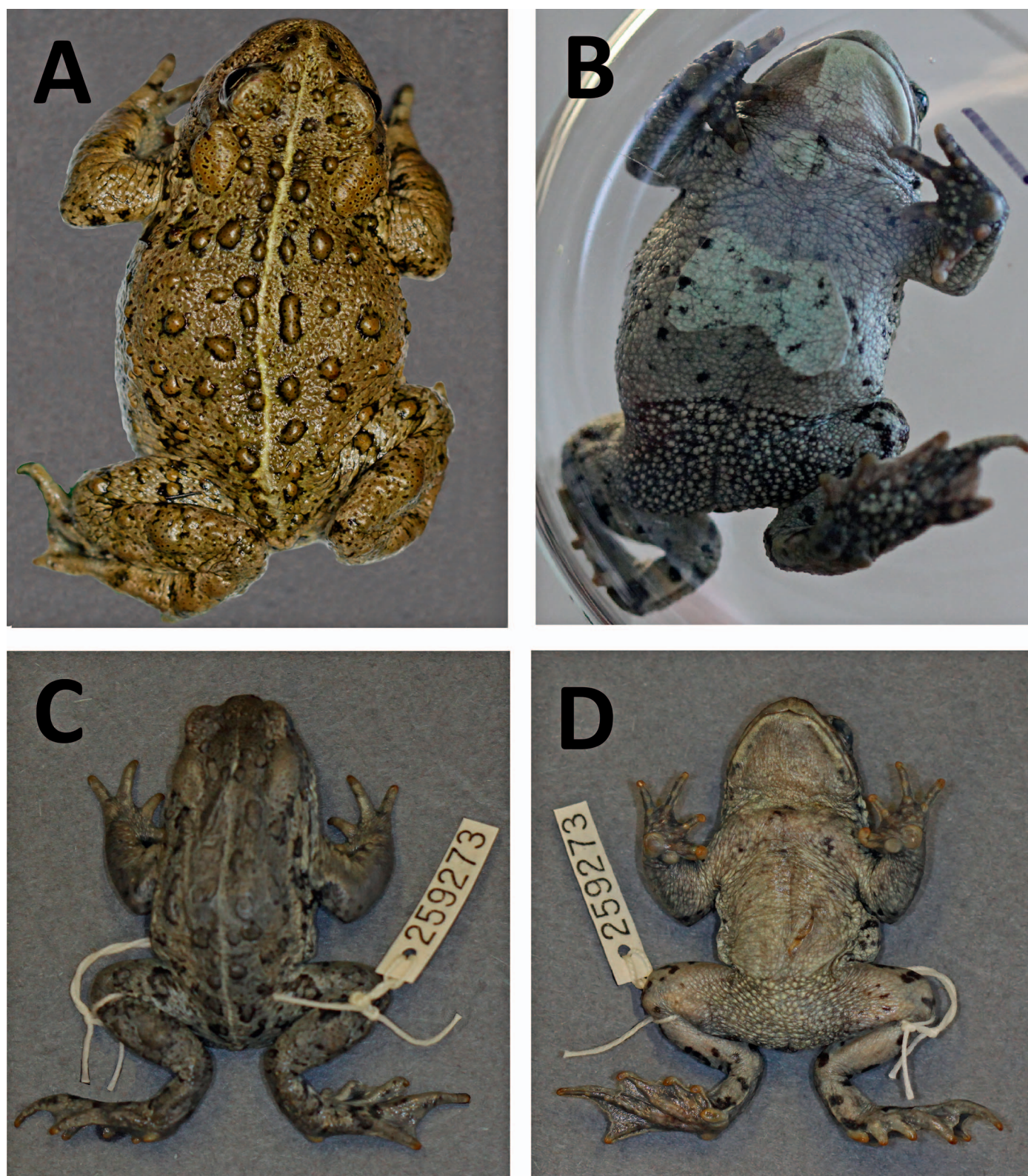


**Fig. 7.** Photographs of *Bufo (Anaxyrus) monfontanus*, new species, holotype (CAS 259273). Male toad in life: (A) dorsal view and (B) ventral view; and in preservative: (C) dorsal view and (D) ventral view. Photographs taken by M. R. Gordon.

metatarsal tubercle pronounced, ovoid. Longitudinally along dorsum, dorsal stripe weakly present, originating posterior to interorbital space, terminating at urostyle; irregular, elevated but scattered warts present, increasing in size from interor-

bital space to posterior margin of urostyle. Skin between warts nearly smooth; forearms smooth; hind limbs exhibit minor warts, tibial gland scarcely present and irregular. Originating posterior to labial commissure, inferior to



tympaum, dense, small tubercles occur along posterior axillary line, terminating near anterior articulation of femur. Venter coarse; seat patch granular and conspicuous.

**Color in life.**—Dorsal background color light olive gray with minor black flecks throughout dorsum; elevated brown warts encircled by narrow, incomplete black border (Fig. 7A). More pronounced black rings border brown warts laterally along posterior axillary line. Dorsal stripe present; fine line, light green, interrupted at parotoid region. Pupils horizontal; iris flecked gold. Parotoid glands flecked with black, minute spots against olive gray. Thick brown stripe present, inferior to eye, occurring from orbit anterior border down to upper lip margin; buffy colored tubercles originate at labial commissure, transition to more olive colored spines moving laterally along body. Along midaxillary line, olive background color transitions to cream color with heavy black blotching. Throat clear, buffy colored. Venter nearly clear, buffy with minor black spots except at seat patch, which is gray and coarse with fine white granules (Fig. 7B). Dorsally, forelimbs exhibit little color variation from olive with some minor dark brown patches; hind limbs have minor black stripes atop white background color along inner shank down to dorsal side of foot.

**Variation.**—In paratypes, dorsal stripe present or weakly present; dorsum ground color variable shades of olive; venter may exhibit minor black spotting against buffy ventral ground color. Parotoids directed parallel behind eyes or slightly convergent at posterior ends. Brown striping above lip and inferior to eyes may be weakly present.

**Color in preservative.**—There are notable differences in preservation (Fig. 7C, D) when compared in life (Fig. 7A, B). Overall ground color of preserved holotype is dark and gray. Dorsal stripe thin, white, broken at posterior edges of parotoid glands, continues to vent. Warts along dorsum flattened, dark gray, and similar in shade to ground color and parotoid glands. Head dark gray, striping inferior to eye muted and tubercles posterior to labial commissure appear white. Arms very smooth and dark. Nuptial pads present and brown in preservative. Marbling along midaxillary line black against muted gray ground color. Venter light gray overall; seat patch muted in preservative. Tubercles on feet and hands diminished and dark, tips appear brown.

**Distribution.**—*Bufo monfontanus* is only found within the marshes fed by thermal spring outflows in Hot Creek Canyon (1,859 m above sea level) in Hot Creek Range in Central Nevada. The narrow canyon is nestled between Box and Corral Canyons and runs east to west, and toads have only been found in the small Hot Creek stream fed by Upper Warm Springs. This locality is extremely remote and isolated, and the spring flows through the canyon are interrupted, likely restricting toad dispersal from east to west, with few suitable corridors outside the canyon. The estimated range for *B. monfontanus* is extremely small at 1 km<sup>2</sup>, as essential wetland habitat is critically limited and isolated by cold desert habitat dominated by sagebrush steppe. The population size is unknown for this endemic toad, but is likely small and warrants further examination. *Bufo monfontanus* co-occurs with introduced *Crenichthys nevadae* (Railroad Valley Spring-fish) near Upper Warm Springs, and the introduced *Rana*

*catesbeiana* (American Bullfrog) can be found within the interior streams of the canyon.

**Life history and behavior.**—*Bufo monfontanus* emerges only after dusk, exhibiting typical nocturnal behavior similar among taxa of the *B. boreas* species complex with the exception of *B. canorus*, which is diurnal. This species can be found in the marshy water or in the perimeter band that transition from riparian habitat to sagebrush steppe. Typical of other species in the *B. boreas* species complex, *B. monfontanus* likely hibernates, using burrows. Little is known about the dispersal behavior of this toad. The high elevation and extreme temperatures, both daily and season-to-season variability, likely prohibit a long breeding season, and further investigation through monitoring and annual surveys could provide insight into the life history strategy of this unique toad.

**Etymology.**—The species name *monfontanus* (from the Latin “mons” for mountain and Latin “fons,” a spring or fountain) is descriptive of the high-elevation spring habitat where this toad occurs and pays tribute to the nature of the rare spring habitat and the biodiversity relying on this important resource within the Nevada.

**Remarks.**—This new toad species, similar to other taxa of the *B. boreas* species complex, represents another narrow endemic that is found only in small and fragile spring ecosystems of the Great Basin. This new species warrants high conservation concern and urgent initiatives to monitor and to study how to preserve this new toad species. Especially troubling is that little is known about the population size, breeding, and dispersal of this small toad species. Additionally, the predatory generalist *Rana catesbeiana* co-occurs within the spring-fed stream system of Hot Creek Canyon, and this species is known to outcompete and prey upon much smaller anurans such as bufonids. *Rana catesbeiana* is also a known vector for potentially lethal anuran diseases, such as chytridiomycosis (Kats and Ferrer, 2003; Daszak et al., 2004), whose effects on the narrowly distributed *B. monfontanus* is unknown.

## DISCUSSION

Our combined genetic and comparative morphological evidence strongly support recognizing two newly described toads, *B. nevadensis* and *B. monfontanus*, increasing the diversity of the Great Basin *B. boreas* complex to seven species. Taxonomic nomenclature within the Nearctic genus *Bufo* remains unstable, so we recommend retaining the two new species in the genus *Bufo*, with *Anaxyrus* used at the subgeneric rank (Pauly et al., 2009). The descriptions of these two new species bring the number of species of *Anaxyrus* to 25 (Pauly et al., 2009; Frost, 2015). These new species are morphologically distinct (Table 1) and genetically differentiated (Fig. 3) from the broadly distributed *B. boreas*, as well as from each other, adding to the intricate phylogeographic story of the *B. boreas* complex of the arid Great Basin. *Bufo nevadensis* and *B. monfontanus* are seemingly close in geographic proximity, separated by approximately 61 km of mountainous desert landscape, yet both have evolved unique phenotypic traits that are nearly opposite of each other in some respects. *Bufo nevadensis*, found only a small locality within Railroad Valley, Nye County, Nevada, is overall squat

and warty, but with dramatically diminished parotoid glands (Fig. 6A, C), while the relatively high elevation toad, *B. monfontanus* of Hot Creek Canyon, Nye County, Nevada, which is nestled in the mountains of Hot Creek Range, exhibits relatively large, close-set parotoid glands and a weakly warted, comparatively slender body (Figs. 6C, 7A). Additionally, sexual dimorphism was only detected for *B. monfontanus*. While MANCOVA analyses are robust to uneven sample sizes, further analysis of a larger sample of *B. nevadensis* males may uncover sexual variation among *B. nevadensis*. The life histories for both of these newly named species warrants serious attention as the population numbers are unknown, and the geographic ranges for these species are among the smallest known among the taxa of the *B. boreas* species complex. Breeding and reproduction timing have been documented in *B. nevadensis*, but not in *B. monfontanus*. However, this may be due to phenological differences in the species due to extreme dissimilarities in temperature and weather experienced by the mountain-inhabiting *B. monfontanus*. These parameters may limit the reproductive window, akin to the environmental restrictions experienced by *B. canorus* (Karlstrom, 1962), a narrowly distributed high elevation relative found only in the Sierra Nevada Mountains (Fig. 5B). Despite a strong difference in habitat elevation, both *B. nevadensis* and *B. monfontanus* rely on rare spring-fed wetlands, a habitat that is often a small and isolated aquatic resource within the state of Nevada, a region that comprises much of the interior of the arid Great Basin Desert (Sada and Vinyard, 2002). Although scarce, these riparian habitats are important hubs supporting widespread biodiversity and are often identified as sites rich in endemism, demonstrated by the high taxonomic diversity of spring fish (Hubbs and Miller, 1948; Hewitt, 1996, 2000; Smith et al., 2002; Finger and May, 2015), spring snails (Hershler and Sada, 2002; Sada and Vinyard, 2002), riparian insects (Shepard, 1992) and toads (Wang, 2009; Gordon et al., 2017). While new species within the region have been recognized, undetected and cryptic diversity is still likely within the region as many of these aquatic resources are difficult to detect, severely isolated (Shepard, 1993), and rarely studied.

The Great Basin *B. boreas* species complex presents an ideal vehicle for evolutionary study demonstrated by the recent discoveries of cryptic species *B. williamsi* (Gordon et al., 2017) and the two new species described here. While neither species is sympatric with *B. boreas*, these divergent lineages represent new evolutionary trajectories from a common ancestor shared with the western toad, which is supported by molecular evidence (Fig. 3, Table 5) and emphasized by the variations exhibited in morphology by the region's toad species (Fig. 5B). The Great Basin Desert may appear to be an unlikely setting for new bufonid species, as amphibians are among the rarest animals to occur within this region. However, the occurrence of this species complex, whose localized endemics are confined to extremely restricted ranges within this exceptionally dry ecoregion, continues to spur study examining range-wide diversity of *B. boreas* to gain insight into the evolutionary relationships among these close relative toads (Graybeal, 1993; Stephens, 2001; Goebel, 2005; Goebel et al., 2009; Switzer et al., 2009). An interesting result from our molecular study suggests that *B. nevadensis* and *B. monfontanus* are more closely related to western toads in Colorado (*B. nevadensis*) and Utah (*B. monfontanus*). In the work of Goebel et al. (2009), genetic analyses suggested that there were

divergent lineages of *B. boreas* uncovered in the phylogenetic analyses from both states, but morphology was not investigated. Research examining the historic hydrological connections into Railroad Valley suggests a connection from the now disjunct White River to the Colorado River, which may have provided the corridors necessary for toad dispersal into the southern Great Basin (Noles, 2010). This may provide some explanation for the high level of divergence exhibited in *B. nevadensis* and *B. monfontanus* to Great Basin *B. boreas* and allied taxa (Table 5), and elucidate the genetic link to western toads outside the region. Additional study is required to advance our understanding of the fine-scale relationships among the toads within this species complex and work to identify cryptic taxa that may still remain undetected under the broad range of the Western Toad.

As species are fundamental to biological study, accurate taxonomy is critical for proper evaluation of diversity and conservation implementation (Bickford et al., 2007). *Bufo nevadensis* and *B. monfontanus* represent novel species concealed within a widely distributed nominal species (Bickford et al., 2007). These species went undetected until our recent molecular study, which demonstrates the increased risk of extinction for cryptic species that are rare due to inadequately resolved taxonomy. With the exception of widely distributed *B. boreas*, the congeneric taxa of the *B. boreas* species complex are currently Threatened (IUCN, 2015) and themselves restricted to extremely small ranges (Fig. 5B). Both *B. nevadensis* and *B. monfontanus* inhabit severely small geographic distributions and join this complex as critically imperiled new members of the *B. boreas* species complex. This study exposes the link between taxonomic cryptic species and high extinction risk, which can have profound consequences to the preservation of biodiversity due to inaccurate taxonomy that may result in improper conservation initiatives. Inadequate conservation can result in serious ramifications, which further endanger these rare, endemic toads reliant on rare, isolated, and fragile wetland habitat open to mismanagement. Unknown population sizes, limited knowledge of life histories, and small geographic ranges further emphasize the increased risk of extinction for both these newly discovered bufonids. Moreover, these new toad species reveal that our knowledge of North American anuran diversity remains incomplete (Bickford et al., 2007; Crawford et al., 2010), and taxonomic cryptic species among frogs poses an important challenge in preservation of anuran diversity and conservation for a class experiencing global declines and extinctions (Collins and Storer, 2003; Corn, 2005; Köhler et al., 2005; Crawford et al., 2010; Lannoo, 2012). Delimiting both *B. monfontanus* and *B. nevadensis* is the first step in refining our knowledge of the diversity within the *B. boreas* species complex, enriching our understanding of bufonid evolution within the Great Basin, and is the necessary first step in launching critical conservation initiatives to protect these vulnerable, rare toads.

#### DATA ACCESSIBILITY

Supplemental material is available at <https://www.copeiajournal.org/ch-18-086>.

#### ACKNOWLEDGMENTS

We would like to extend our gratitude to US Fish and Wildlife Service (especially Bob Williams and Todd Gilmore), the



Biological Resources Research Center, and the Department of Biology of the University of Nevada, Reno for providing funding for this research. Further thanks are extended for the invaluable field support from Sarah Snyder and Molly Betchel, plus field assistance from Kevin Guadalupe and Chris Burg of Nevada Department of Wildlife (NDOW #223071); laboratory support and genetic modeling from Bridgette Hagerty; Molly Stephens for bufonid tissues used to develop DNA markers; assistance in phylogenetic reconstruction from Joshua Hallas, Mo Beck, and Matthew Forister; and aid from Pete Noles and Erich Purpur on map development and design. We extend thanks to Chris Feldman for his help in preserving the holotype and the paratypic series. Additional thanks to Jens Vindum for assistance with the deposition of the valuable specimens into the Herpetology Department of the California Academy of Sciences. We were grateful for thoughtful reviews and attention to detail on early drafts from Chava Weitzman.

# LITERATURE CITED

- Avise, J. C., J. Arnold, R. M. Ball, E. Bermingham, T. Lamb, J. E. Neigel, C. A. Reeb, and N. C. Saunders. 1987. Intraspecific phylogeography: the mitochondrial DNA bridge between population genetics and systematics. *Annual Reviews of Ecological Systems* 18:459–522.
- Bickford, D., D. J. Lohman, S. S. Navjot, P. K. L. Ng, R. Meier, K. Winker, K. K. Ingram, and I. Das. 2007. Cryptic species as a window on diversity and conservation. *Trends in Ecology and Evolution* 22:148–155.
- Blair, F. W. 1972. *Evolution of the Genus Bufo*. University of Texas Press, Austin, Texas.
- Burnham, K. P., and D. R. Anderson. 2002. *Model Selection and Multimodel Inference: A Practical Information-theoretic Approach*. Springer, New York.
- Clement, M., Q. Snell, P. Walke, D. Posada, and K. Crandall. 2002. TCS: estimating gene genealogies. *Proceedings of the 16<sup>th</sup> International Parallel Distributing Processing Symposium* 2:184.
- Collins, J. P., and A. Storfer. 2003. Global amphibian declines: sorting the hypotheses. *Diversity and Distribution* 9:89–98.
- Corn, P. S. 2005. Climate change and amphibians. *Animal Biodiversity and Conservation* 28:59–67.
- Crawford, A. J., K. R. Lips, and E. Bermingham. 2010. Epidemic disease decimates amphibian abundance, species diversity, and evolutionary history in the highlands of central Panama. *Proceedings of the National Academy of Sciences of the United States of America* 107:13777–13782.
- Dahl, J., and B. L. Peckarsky. 2002. Induced morphological defenses in the wild: predator effects on a mayfly, *Drunella coloradensis*. *Ecology* 83:1620–1634.
- Daszak, P., A. Strieby, A. A. Cunningham, J. E. Longcore, C. C. Brown, and D. Porter. 2004. Experimental evidence that the bullfrog (*Rana catesbeiana*) is a potential carrier of chytridiomycosis, an emerging fungal disease of amphibians. *Herpetological Journal* 14:201–207.
- Feder, J. H. 1973. Genetic variation and biochemical systematics in western *Bufo*. Unpubl. master's thesis. University of California, Berkeley, California.
- Feinberg, J. A., C. E. Newman, G. J. Watkins-Colwell, M. D. Schlesinger, B. Zarate, B. R. Curry, H. B. Shaffer, and J. Burger. 2014. Cryptic diversity in Metropolis: confirmation of a new leopard frog species (Anura: Ranidae) from New York City and surrounding Atlantic coast regions. *PLoS ONE* 9:e108213.
- Felsenstein, J. 1985. Confidence limits on phylogenies: an approach using the bootstrap. *Evolution* 39:783–791.
- Finger, A. J., and B. May. 2015. Conservation genetics of a desert fish species: the Lahontan tui chub (*Siphateles bicolor* ssp.). *Conservation Genetics* 16:743–758.
- Frost, D. R. 2015. *Amphibian Species of the World: an Online Reference*. Version 6.0 American Museum of Natural History, New York. Available from <http://research.amnh.org/herpetology/amphibia/index.html> (accessed 9 December 2015).
- Goebel, A. M. 1996. Systematics and conservation of bufonids in North America and in the *Bufo boreas* species group. Unpubl. Ph.D. diss., University of Colorado at Boulder, Colorado.
- Goebel, A. M. 2005. Conservation systematics: the *Bufo boreas* species group, p. 210–221. In: *Amphibian Declines: The Conservation Status of United States Species*. M. J. Lannoo (ed.). University of California Press, Berkeley, California.
- Goebel, A. M., J. M. Donnelly, and M. E. Atz. 1999. PCR primers and amplification methods for 12S ribosomal DNA, the control region, cytochrome oxidase I, and cytochrome *b* in bufonids and other frogs, and an overview of PCR primers which have amplified DNA in amphibians successfully. *Molecular Phylogenetics and Evolution* 11:163–199.
- Goebel, A. M., T. A. Ranker, P. S. Corn, and R. G. Olmstead. 2009. Mitochondrial DNA evolution in the *Anaxyrus boreas* species group. *Molecular Phylogenetics and Evolution* 50:209–225.
- Gordon, M. R., E. T. Simandle, and C. R. Tracy. 2017. A diamond in the rough, desert shrublands of the Great Basin, western United States: a new cryptic toad species (Amphibia: Bufonidae *Bufo* (*Anaxyrus*)) uncovered from northern Nevada. *Zootaxa* 4290:123–139.
- Graybeal, A. 1993. The phylogenetic utility of cytochrome *b*: lessons from bufonid frogs. *Molecular Phylogenetics and Evolution* 2:256–269.
- Hasegawa, M., H. Kishino, and T. Yano. 1985. Dating of the human-ape splitting by a molecular clock of mitochondrial DNA. *Journal of Molecular Evolution* 22:160–174.
- Hayek, L. C., W. R. Heyer, and C. Gascon. 2001. Frog morphometrics: a cautionary tale. *Alytes* 18:153–177.
- Hershler, R., and D. W. Sada. 2002. Biogeography of Great Basin aquatic snails of the genus *Pyrgulopsis*, p. 255–276. In: *Great Basin Aquatic Systems History: Smithsonian Contributions to the Earth Sciences, Number 33*. R. Hershler, D. B. Madsen, and D. R. Currey (eds.). Smithsonian Institution Press, Washington, D.C.
- Hewitt, G. M. 1996. Some genetic consequences of ice ages, and their role in divergence and speciation. *Biological Journal of the Linnean Society* 58:247–276.
- Hewitt, G. M. 2000. The genetic legacy of the quaternary ice ages. *Nature* 405:907–913.
- Hubbs, C. L., and R. R. Miller. 1948. The zoological evidence: correlation between fish distribution and hydrographic history in the desert basins of western United States. *Bulletin of the University of Utah* 38:17–166.

- IUCN. 2015. The IUCN Red List of Threatened Species. Version 2015–3. <https://www.iucnredlist.org> (accessed 9 September 2015).
- Jukes, T. H., and C. R. Cantor. 1969. Evolution of protein molecules, p. 21–132. *In*: Mammalian Protein Metabolism. H. N. Munro (ed.). Academic Press, New York.
- Karlstrom, E. L. 1962. The toad genus *Bufo* in the Sierra Nevada of California: ecological and systematic relationships. University of California Publications in Zoology 62: 1–104.
- Kats, L. B., and R. P. Ferrer. 2003. Alien predators and amphibian declines: review of two decades of science and the transition to conservation. Diversity and Distributions Journal 9:99–110.
- Köhler, J., D. R. Vieites, R. M. Bonett, F. H. García, F. Glaw, D. Steinke, and M. Vences. 2005. New amphibians and global conservation: a boost in species discoveries in a highly endangered vertebrate group. BioScience 55:693–696.
- Kumar, S., G. Stecher, and K. Tamura. 2016. MEGA7: Molecular Evolutionary Genetics Analysis version 7.0. Molecular Biology and Evolution 33:1870–1874.
- Lannoo, M. J. 2012. A perspective on amphibian conservation in the United States. Alytes 29:133–144.
- Larkin, M. A., G. Blackshields, N. P. Brown, R. Chenna, P. A. McGettigan, H. McWilliam, F. Valentin, I. M. Wallace, A. Wilm, R. Lopez, J. D. Thompson, T. J. Gibson, and D. G. Higgins. 2007. Clustal W and Clustal X version 2.0. Bioinformatics 23:2947–2948.
- Leigh, J. W., and D. Bryant. 2015. POPART: full-feature software for haplotype network construction. Methods in Ecology and Evolution 6:1110–1116.
- Liu, X., U. Fehn, and R. T. D. Teng. 1997. Oil formation and fluid convection in Railroad Valley, NV: a study using cosmogenic isotopes to determine the onset of hydrocarbon migration. Nuclear Instruments and Methods in Physics Research B 123:356–360.
- Lleonart, J., J. Salat, and G. J. Torres. 2000. Removing allometric effects of body size in morphological analysis. Journal of Theoretical Biology 205:85–93.
- McCoy, M. W., B. M. Bolker, C. W. Osenberg, B. G. Miner, and J. R. Vonesh. 2006. Size correction: comparing morphological traits among populations and environments. Oecologia 148:547–554.
- Noles, P. M. 2010. Reconciling western toad phylogeography with Great Basin prehistory. Unpubl. M.S. thesis, University of Nevada, Reno, Nevada.
- Pattengale, N. D., M. Alipour, O. R. P. Bininda-Emonds, B. M. E. Moret, and A. Stamatakis. 2010. How many bootstrap replicates are necessary? Journal of Computational Biology 17:337–354.
- Pauly, G. B., D. M. Hillis, and D. C. Cannatella. 2004. The history of a Nearctic colonization: molecular phylogenetics and biogeography of the Nearctic toads (*Bufo*). Evolution 58:2517–2535.
- Pauly, G. B., D. M. Hillis, and D. C. Cannatella. 2009. Taxonomic freedom and the role of official lists of species names. Herpetologica 65:115–128.
- Rambaut, A. 2014. FigTree v1.4.2. <http://tree.bio.ed.ac.uk/software/figtree/>
- Rambaut, A., M. A. Suchard, D. Xie, and A. J. Drummond. 2014. Tracer v1.6. <http://beast.bio.ed.ac.uk/Tracer>
- Ronquist, F., and J. P. Huelsenbeck. 2003. MrBayes 3: Bayesian phylogenetic inference under mixed models. Bioinformatics 19:1572–1574.
- Sada, D. W., and G. L. Vinyard. 2002. Anthropogenic changes in biogeography of Great Basin aquatic biota, p. 277–293. *In*: Great Basin Aquatic Systems History: Smithsonian Contributions to the Earth Sciences, Number 33. R. Hershler, D. B. Madsen, and D. R. Currey (eds.). Smithsonian Institution Press, Washington, D.C.
- Shaffer, H. B., G. M. Fellers, A. Magee, and S. R. Voss. 2000. The genetics of amphibian declines: population substructure and molecular differentiation in the Yosemite Toad, *Bufo canorus* (Anura, Bufonidae) based on single-strand conformation polymorphism analysis (SSCP) and mitochondrial DNA sequence data. Molecular Ecology 9:245–257.
- Shepard, W. D. 1992. Riffle beetles (Coleoptera: Elmidae) of Death Valley National Monument, California. Great Basin Naturalist 52:378–381.
- Shepard, W. D. 1993. Desert springs—both rare and endangered. Aquatic Conservation: Marine and Freshwater Ecosystems 3:351–359.
- Smith, G. R., T. Dowling, K. W. Gobalet, T. Lugaski, D. Shiazawa, and R. P. Evans. 2002. Biogeography and timing of evolutionary events among Great Basin fishes, p. 175–234. *In*: Great Basin Aquatic Systems History: Smithsonian Contributions to the Earth Sciences, Number 33. R. Hershler, D. B. Madsen, and D. R. Currey (eds.). Smithsonian Institution Press, Washington, D.C.
- Stebbins, R. C. 2003. Peterson Field Guide to Western Reptiles and Amphibians. Third edition. Houghton Mifflin Company, Boston.
- Stephens, M. R. 2001. Phylogeography of the *Bufo boreas* (Anura, Bufonoidea) species complex and the biogeography of California. Unpubl. M.A. thesis, Sonoma State University, Rohnert Park, California.
- Switzer, J. F., R. Johnson, B. A. Lubinski, and T. L. King. 2009. Genetic structure in *Anaxyrus boreas* species group (Anura, Bufonidae): an evaluation of the Southern Rocky Mountain population. United States Fish and Wildlife Report, Mountain-Prairie Region.
- Wang, I. J. 2009. Fine-scale population structure in a desert amphibian: landscape genetics of the black toad (*Bufo exsul*). Molecular Ecology 18:3847–3856.